

AD-A032 366

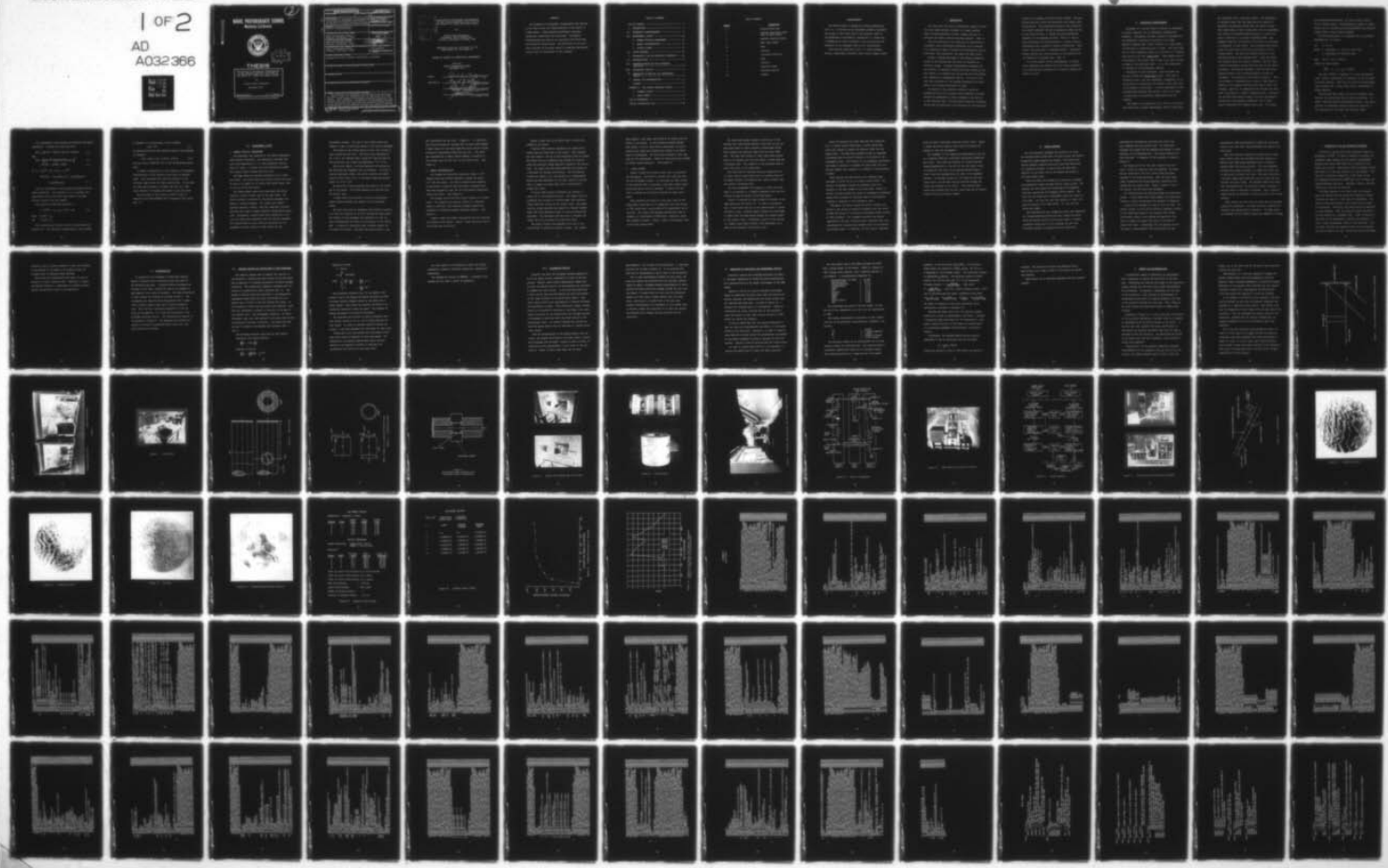
NAVAL POSTGRADUATE SCHOOL MONTEREY CALIF
APPLICATION OF HOLOGRAPHIC INTERFEROMETRY TO THE INTERIOR BALLI--ETC(U)
SEP 76 R L MONTGOMERY

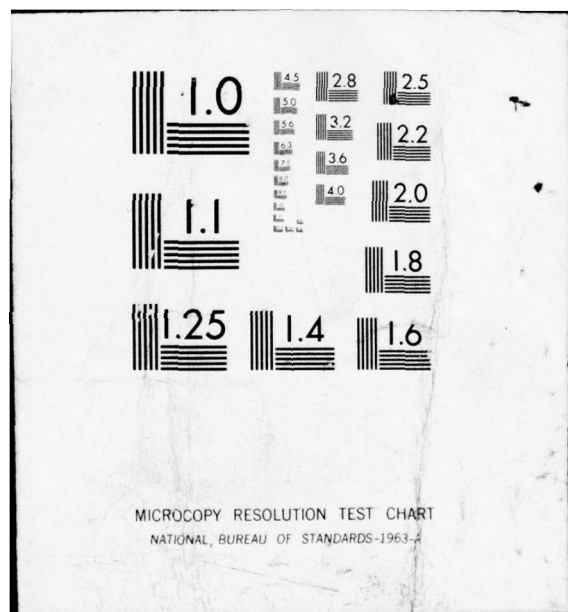
F/G 20/6

UNCLASSIFIED

1 OF 2
AD
A032366

NL





MICROCOPY RESOLUTION TEST CHART
NATIONAL BUREAU OF STANDARDS-1963-A

(2)
NW
AD A032366

NAVAL POSTGRADUATE SCHOOL

Monterey, California



D D C
REF ID: A65114
NOV 23 1976
B

THESIS

APPLICATION OF HOLOGRAPHIC INTERFEROMETRY
TO THE INTERIOR BALLISTIC FLOW FIELD IN
THE BARREL OF A TWENTY MILLIMETER CANNON

by

Richard Lewis Montgomery

September 1976

Thesis Advisor:

D. J. Collins

Approved for public release; distribution unlimited.

REPORT DOCUMENTATION PAGE		READ INSTRUCTIONS BEFORE COMPLETING FORM
1. REPORT NUMBER <i>(6)</i>	2. GOV'T ACCESSION NO.	3. RECIPIENT'S CATALOG NUMBER <i>(9)</i>
4. TITLE (and subtitle) Application of Holographic Interferometry to the Interior Ballistic Flow Field in the Barrel of a Twenty Millimeter Cannon		5. TYPE OF REPORT & PERIOD COVERED Master's Thesis, September 1976
7. AUTHOR(s) Richard Lewis / Montgomery		6. PERFORMING ORG. REPORT NUMBER
9. PERFORMING ORGANIZATION NAME AND ADDRESS Naval Postgraduate School Monterey, California 93940		10. PROGRAM ELEMENT, PROJECT, TASK AREA & WORK UNIT NUMBERS <i>(12) 98P.</i>
11. CONTROLLING OFFICE NAME AND ADDRESS Naval Postgraduate School Monterey, California 93940		12. REPORT DATE <i>(11) September 1976</i>
14. MONITORING AGENCY NAME & ADDRESS (if different from Controlling Office) Naval Postgraduate School Monterey, California 93940		13. NUMBER OF PAGES <i>99</i>
16. DISTRIBUTION STATEMENT (of this Report) Approved for public release; distribution unlimited.		15. SECURITY CLASS. (of this report) Unclassified
17. DISTRIBUTION STATEMENT (of the abstract entered in Block 20, if different from Report)		15a. DECLASSIFICATION/DOWNGRADING SCHEDULE
18. SUPPLEMENTARY NOTES		
19. KEY WORDS (Continue on reverse side if necessary and identify by block number)		
20. ABSTRACT (Continue on reverse side if necessary and identify by block number) The technique of holographic interferometry was applied to the study of gas core characteristics in the barrel of a 20mm cannon. Using standard hydrodynamic equations theoretical predictions were calculated. Holographic interferograms were made of the associated flow field near the projectile during firing. Reconstruction of the wavefront provided the necessary means of comparing experimental results with the theoretical values obtained.		

PROFESSIONAL	
OTIS	With Solder
OTC	With Solder <input checked="" type="checkbox"/>
UNARMED	
JUSTIFICATION	
BY	
DISTRIBUTION/AVAILABILITY CODES	
DISL	ALAR, AND OR OFICIAL
A	

Application of Holographic Interferometry
to the Interior Ballistic Flow Field in
the Barrel of a Twenty Millimeter Cannon

by

Richard Lewis Montgomery
Lieutenant, United States Navy
B.S.E.E., University of Miami, 1966

Submitted in partial fulfillment of the
requirements for the degree of

MASTER OF SCIENCE IN AERONAUTICAL ENGINEERING

from the

NAVAL POSTGRADUATE SCHOOL
September 1976

Author

Richard Lewis Montgomery

Approved by:

Daniel J. Collins

Thesis Advisor

Edward W. Reed

Chairman, Department of Aeronautics

J. M. Beusterien

Academic Dean

ABSTRACT

The technique of holographic interferometry was applied to the study of gas core characteristics in the barrel of a 20mm cannon. Using standard hydrodynamic equations theoretical predictions were calculated. Holographic interferograms were made of the associated flow field near the projectile during firing. Reconstruction of the wave-front provided the necessary means of comparing experimental results with the theoretical values obtained.

TABLE OF CONTENTS

LIST OF SYMBOLS -----	5
I. INTRODUCTION -----	7
II. HOLOGRAPHIC INTERFEROMETRY -----	9
III. EXPERIMENTAL LAYOUT -----	14
A. GENERAL PHYSICAL ARRANGEMENT -----	14
B. BARREL INSTRUMENTATION -----	16
C. OPTICAL SYSTEM -----	18
IV. FIRING SEQUENCE -----	22
V. HOLOGRAPHIC FILM AND PROCESSING TECHNIQUE -----	25
VI. RECONSTRUCTION -----	27
VII. COMPUTER PROGRAM AND FLOW PARAMETER PREDICTION -----	28
VIII. HOLOGRAPHIC RESULTS -----	31
IX. COMPARISON OF ANALYTIC AND EXPERIMENTAL RESULTS -----	33
X. SUMMARY AND RECOMMENDATIONS -----	37
FIGURES -----	39
APPENDIX A: GUN PROJECT COMPUTER PROGRAM -----	61
A. PROGRAM LISTING -----	61
B. INPUT FORMAT -----	92
LIST OF REFERENCES -----	97
INITIAL DISTRIBUTION LIST -----	98

LIST OF SYMBOLS

<u>SYMBOL</u>	<u>DEFINITION</u>
A	Cross-section area
C	Constant specifying thickness of shock region
E	Specific internal energy
j	Mass point number
M	Mass
P	Pressure
q	Artificial viscosity
t	Time
u	Velocity
v	Specific Volume
x	Eulerian Position
ρ	Density

ACKNOWLEDGMENT

The Author wishes to express his sincere appreciation to Dr. D. J. Collins for his invaluable guidance throughout the course of this study, and to the technical staff of the Department of Aeronautics, particularly P. Hickey and G. Middleton for their assistance in the construction and operation of the equipment used in this investigation.

This work was sponsored by the U. S. Naval Ordnance Station, Indian Head, Maryland, under Project Number 4-0029.

I. INTRODUCTION

For many years the field of theoretical interior ballistics was almost entirely confined to a single problem: given the characteristics of shot, charge, and gun, to calculate the muzzle velocity and peak pressure. (Ref. 1)

With the discovery of the laser and its application to holography, more interesting information can be obtained. It is possible to make a hologram of the projectile and its flow field, then reconstruct the image with exact detail.

Having a thorough knowledge of the physical characteristics of the internal gas flow field is essential in ballistic design. Although thermochemical constants for the products of combustion during actual gun firing are not well known, it is assumed that the gas and the solid grains move together as a homogeneous mixture. If this is true, then the conclusions of the Lagrange hypothesis are applicable to the interior ballistics of a gun.

The motion of the projectile creates a system of rarefaction waves in the breech, with relaxation occurring through the mechanisms of stress transfer in the bed and in the propellant gas. The dual wave system will accelerate the gas and the particles in the direction of the projectile

motion at the expense of stored internal energy. The more volatile gas will follow the projectile more readily than the particles. With progressive motion of the projectile, the initial unsteady flow may be expected to damp out and, as the motion evolves, to assume the quasi-equilibrium character of the Lagrange solution. This is a flow in which the mixture has uniform density, a linear velocity distribution and a quadratic pressure distribution. Eventually, the propellant is consumed entirely. Subsequent motion involves only the propulsion of the projectile by the reservoir of energetic gas. (Ref. 2)

It is the purpose of this investigation to utilize laser techniques and observe this flow field responsible for propelling the projectile as it transits through the barrel of a gun.

II. HOLOGRAPHIC INTERFEROMETRY

Holography is a process which is similar to photography in certain respects, but is nonetheless fundamentally different. Photography provides a method of recording the two-dimensional irradiance distribution of an image. Generally speaking each "scene" consists of a large number of reflecting or radiating points of light. The waves from each of these elementary points all contribute to a complete wave which we call the "object wave." This complex wave is transformed by the optical lens in such a way that it forms an image of the radiating object. It is this image which is recorded on the photographic emulsion.

Holography is quite different. With holography one actually records the object wave itself. This wave is recorded in such a way that subsequent illumination of the record serves to reconstruct the original object wave even in the absence of the object. A visual observation of this reconstructed wavefront then yields a view of the object or scene which is practically indiscernible from the original.

The method of recording the object wave is as follows. One starts with a single monochromatic beam of light which

has originated from a very small source. The requirement of coherence means that the light should be capable of displaying interference effects that are stable in time. This single beam of light is then split into two components, one of which is directed toward the object or scene; the other is directed to a suitable recording medium. The component beam that is directed to the object is scattered, or diffracted, by that object. This scattered wave constitutes the object wave, which now is directed to the recording medium. The wave that proceeds directly to the recording medium is the reference wave. Since the object and reference waves are mutually coherent, they will form a stable interference pattern when they meet on the recording medium. The detailed permanent record of this interference pattern on the recording medium is called the "hologram." This method is illustrated in Figure 1. When the hologram is illuminated with a beam of light which is similar to the original reference wave used to record the hologram, light will be transmitted only through the clear areas, resulting in a complex transmitted wave. Because of the recorded interference fringes, this wave conveniently divides into three separate components, one of which exactly duplicates the original object wave. By viewing

this reconstructed wavefront, one sees an exact replica of the original object. Three-dimensional images of opaque objects may be reconstructed and photographed from different viewing angles using a single hologram.

The above description of holography can be represented mathematically as follows:

$$\text{Let } \bar{E} = \bar{O} + \bar{R} \quad 2.1$$

Where \bar{O} represents the object or scene beam

\bar{R} represents the reference beam

$$\text{Then } E^2 = O^2 + R^2 + 2\langle \bar{O} \cdot \bar{R} \rangle \quad 2.2$$

Taking the time average:

$$\langle \bar{E}^2 \rangle = I = I_O + I_R + 2\langle \bar{O} \cdot \bar{R} \rangle \quad 2.3$$

The term $2\langle \bar{O} \cdot \bar{R} \rangle$ in equation 2.3 is the interference term. Without interference the intensity of the two beams are merely additive. With the utilization of monochromatic light derived from a single ideal source, interference is always possible.

Uncorrelated light beams, as from two different light sources, are uncorrelated and are called incoherent. Coherent radiation produces interference effects. The superposition of incoherent radiation yields the addition of the intensities of the object and reference beams.

The interference term contains both amplitude and phase information. Consider two waves such that:

$$\bar{O} \cdot \bar{R} = \frac{1}{4} (\bar{O} e^{-i\omega t} + \bar{O}^* e^{i\omega t}) (\bar{R} e^{-i\omega t} + \bar{R}^* e^{i\omega t}) \quad 2.4$$

Then

$$\bar{O} \cdot \bar{R} = \frac{1}{4} \left\{ \bar{O} \cdot \bar{R} e^{-2i\omega t} + \bar{O}^* \bar{R}^* e^{2i\omega t} + \bar{O} \cdot \bar{R}^* + \bar{O}^* \cdot \bar{R} \right\} \quad 2.5$$

$$2 \langle \bar{O} \cdot \bar{R} \rangle = \frac{1}{2} (\bar{O} \cdot \bar{R}^* + \bar{O}^* \cdot \bar{R}) \quad 2.6$$

If $O_1 = O_1 e^{ig_1}$ etc. and $R_1 = r_1 e^{ih_1}$

$$2 \langle \bar{O}_1 \cdot \bar{R}_2 \rangle = O_1 r_1 \cos(g_1 - h_1) + O_2 r_2 \cos(g_2 - h_2) \\ + O_3 r_3 \cos(g_3 - h_3) \quad 2.7$$

Thus the interference term contains both amplitude and phase information. From equation 2.6 it is evident that interference occurs only when light beams of the same polarity interact with one another.

The complete interference equation is:

$$I = \langle \bar{E}^2 \rangle + I_R + I_0 + R \cdot O^* + O \cdot R^* \quad 2.8$$

where $\langle R \cdot R^* \rangle = I_R$

and $\langle O \cdot O^* \rangle = I_0$

The reconstruction process can also be described with equation 2.8. The amplitude transmittance of the hologram

is assumed to be proportional to the intensity

$$t(x) + KI$$

2.9

On reconstruction with the reference beam R, the following is obtained:

$$R \cdot KI = R(I_R + I_0) + R \cdot R \cdot O^* + R \cdot R^* \cdot O \quad 2.10$$

The last term in equation 2.10 is the reconstructed object beam.

A primary consideration in the technique of holographic interferometry of flow fields is the source of coherent light. The Q-switched ruby laser has proved to be an excellent light source for these applications. It provides the high power necessary to expose the plate in a time frame suitable for freezing the motion of the flow field.

The wavelength of this laser is $6943 \text{ } \text{\AA}$, which is compatible with AGFA-GEVAERT 10E75 holographic film plates.
(Ref. 3)

III. EXPERIMENTAL LAYOUT

A. GENERAL PHYSICAL ARRANGEMENT

The experiment was conducted at the Naval Postgraduate School Rocket Laboratory. The laboratory contained four test cells measuring 12' X 17' with reinforced concrete walls 12" thick. A control room with observation windows was located directly behind the test cells.

The 20mm cannon was mounted horizontally on a rocket test stand. Two steel mounts were used to secure the barrel in place at a height of 6.5 inches from barrel center line to the top of the test stand.

Two large wooden tables were constructed and placed parallel to and on either side of the test stand. The tables provided a platform for the optical equipment necessary to obtain holograms. The tables were rigidly fastened together; however, they were completely isolated from the test stand to ensure stability during cannon operation. Furthermore, plywood boxes were constructed to fit over the tables and completely house the optical equipment. The plywood boxes not only acted as protection for the equipment but also acted as a light shield for the

holographic process. The tops of the plywood boxes were hinged in order to allow easy access to the optical equipment.

The muzzle of the cannon faced a bullet trap located 13 feet outside the test cell. The bullet trap contained an 18" X 18" X 1½" armored plate, tilted 45° from the path of the projectile, and a sand trap measuring 5' X 5' X 2½'.

Upon bullet impact, the plate shattered the projectile and deflected the fragments into the sandtrap. In order to provide additional safety, the entire sandtrap was housed inside a steel turret for a 5" gun mount measuring approximately 15' X 20' X 10'.

An electrical firing mechanism was placed at the breech end of the cannon. The firing sequence was directed from the control room.

A light shield was provided to cover the observation window during placement and removal of the holographic plates.

The ruby laser and its components were fixed in position in a test cell adjacent to the cell housing the 20mm cannon. The purpose of this placement was necessary not only for space consideration but mostly for protection of the instrument. A specially constructed table provided support for the laser rail system. The laser was placed normal to the

wall separating the two cells. (Figure 2) A 2-inch hole was drilled through the concrete wall to allow beam passage. A water source for the laser head and output etalon cooling system was incorporated within the test cell. The laser was equipped with a remote control making it possible to fire either from the test cell or the control room. (See Figure 3)

B. BARREL INSTRUMENTATION

For viewing the projectile inside the cannon a .817" diameter hole was drilled completely through the barrel 4.5" from the muzzle. In order to preserve the integrity of the barrel, projectile and flow field, plexiglass windows were designed to seal the port and provide observation inside the barrel. (See Figure 4)

The windows were milled from optical quality 3/4" plexiglass. Two windows were pressure tested in a simulated barrel to 6000 PSI, thus ensuring strength capabilities necessary to withstand internal pressures present. (See Figure 5)

Figure 6 shows the design consideration met for mounting the windows in the barrel. Figure 7 shows the actual barrel with window and with collar.

Figure 8 shows the collar device used to secure the windows in the barrel.

A Kistler 607A pressure transducer was installed 5.5 inches from the breech end of the barrel. This location was just ahead of the tip of the projectile prior to firing. The signal from the transducer was relayed to a Kistler model 504 universal charge amplifier located in the control room. The signal from the charge amplifier was passed to a Textronix 549 storage oscilloscope. The oscilloscope allowed the signal to be time delayed by a predetermined amount and then amplified to +30 volts, which in turn was used to trigger the xenon flash tube of the Korad K-1 pulsed ruby laser.

A Kistler 603H pressure transducer was located 2.5 inches aft of the observation ports. The signal from the transducer was relayed to a Kistler model 504A universal charge amplifier located in the control room. The signal from the charge amplifier was passed to a Hewlett Packard Model 214A pulse generator where it could be delayed and amplified. The resulting pulse was used to energize the Pockel cells of the Korad K-1 pulsed ruby laser.

The muzzle velocity was measured by the use of two Oehler Model 55 ballistic velocity screens. The screens

were mounted 4 feet apart and placed 81.25 inches from the muzzle of the cannon. As the projectile passed through each screen a 12-volt pulse with an adjustable 2-8 millisecond pulse length was produced and relayed to an Oehler Model 21 chronograph. The two pulses provided a start and stop for the chronograph. Tables of velocities were provided for known screen separation. (See Figure 9)

C. OPTICAL SYSTEM

Figure 10 shows the optical layout used to accomplish the holography. The Korad K-1 pulsed ruby laser was used for the holography process. By utilizing the laser system in the Q-switch mode of operation, high power single transverse mode output could be obtained. A Pockel cell was used to achieve the Q-spoiling required for peak output power.

When operating the Korad K-1 pulse ruby laser in the TEM_{00} mode a peak power of 2.5 megawatts with pulse energy of .050 joules over a pulse width of 20 nanoseconds can be realized. The output beam measured approximately 2mm in diameter at a wavelength of 6943\AA° with a coherence length that exceeds one meter. Figure 3 shows a photographic view of the laser installation.

The laser beam passes through a 2-inch hole in the concrete wall then through another 2-inch hole in the plywood boxes where it first contacts a narrow-band filter which removes the undesired light from the xenon flash tube. The beam then strikes a 2-inch round beam splitter where it is divided into two wave fronts, a scene beam and a reference beam. The intensity of the reference beam is about twice that of the scene beam.

The scene beam is directed along the centerline of a 2.5 meter optical bench where prior to striking mirror #1 it passes through a collimating lens, double concave lens and another collimating lens.

The lens arrangement was designed to allow the scene beam to be expanded to a diameter compatible with the hole drilled through the barrel of the 20mm cannon.

Mirror #1 directed the beam through the windows in the 20mm cannon and onto mirror #2. In order to accomplish this, 3-inch holes were cut in the plywood boxes to permit the beam to pass, allowing enough tolerance for adjustment to ensure that the beam passed through the windows normal to the cannon's axes. Furthermore, mirror #1 was secured to a gimbal mount which allowed a fine adjustment to be made in the horizontal and vertical axes.

Mirror #2 directed the scene beam down the centerline of a 1.5 meter optical bench where a second narrow-band filter was located to remove the unwanted flash from the cannon blast. The beam then proceeds through an expanding collimating lens to mirror #3 where it is directed to the holographic plate. The location of the expanding collimating lens makes it possible to enlarge the scene beam from test section (window size) diameter to a diameter of approximately 4-inches.

After passing the beam splitter the reference beam proceeded to mirror #4 on a 2.0 meter optical bench. The physical arrangement allowed the reference beam to be adjusted to the same length as the scene beam. Mirror #5 directs the beam through two series of expanding--collimating lenses which enlarged the reference beam to approximately 4-inches in diameter at the holographic plate.

Throughout the entire system the optical benches were bolted to the tables on specially designed cross feet which allowed the system to be leveled by adjustment knobs located at each crossfoot. The alignment procedure was greatly simplified by the use of mirrors which contained screw type adjustments for vernier-scale movement about the horizontal and vertical axes. In addition, all the optical components

could be easily positioned along the optical bench. Figure 11 shows the actual optical layout with one plywood box removed to show the arrangement.

The alignment of the system was accomplished by the use of a coherent radiation 3-milliwatt helium-neon continuous wave laser. This laser was mounted on a stand which was placed perpendicular to the axis of the ruby laser cavity. By firing the ruby laser on an exposed polaroid paper a "spot" could be obtained which was used in the alignment process. By placing a mirror at a 45° angle in the ruby laser cavity, the CW beam could be directed through the cavity and centered on the "spot." This centered beam would then coincide with the ruby laser beam and the optical system could be accurately aligned.

IV. FIRING SEQUENCE

All the electrical equipment was turned on to allow the required warm-up time while the test section and optical system were being prepared and aligned. The barrel test section assembly required particular care when installing the plexiglass windows, to ensure that the faces were parallel to the center line of the cannon and normal to the laser beam's path.

After the system was aligned, all electrical equipment was checked for proper settings and all timers zeroed. The opening into the plywood box containing the holographic plate was covered and the alignment mirror removed. The test cell was closed and a holographic plate was placed in its holder. The test cell door was raised to a level just above the muzzle of the 20mm cannon. At this time the cannon was loaded.

The individual who was loading the cannon and connecting the firing mechanism carried with him a safety key which broke the firing circuit at the control panel to prevent accidental firing prior to his clearing the test area. Following loading, the opening into the plywood box

containing the hologram was uncovered and control was then commenced from the control room. All electrical equipment was scanned and the warning horn sounded to alert personnel of the impending shot. The firing sequence was then initiated. A schematic of this sequence is shown in Figure 12.

The charge switch for the laser capacitor was activated. While the capacitor bank was charging, the safety key was installed in the fire control panel and power supplied to the firing mechanism. When the laser ready light illuminated the firing mechanism, capacitors were charged and the cannon fired. Figure 13 shows a view of the control room and monitoring equipment.

The firing process was observed through the observation window. A light shield was placed against the window after firing to protect the hologram from unwanted illumination.

Actual bullet movement was used to fire the laser. On initial firing, a pulse from the Kistler transducer located at the breech was passed to the Textronix 549 storage oscilloscope, where it was delayed and amplified, then used to trigger the xenon flash tube of the Korad K-1 pulsed ruby laser. Considering that the pumping time for the laser is approximately 1000 microseconds and that

approximately 1500 microseconds are needed for projectile travel to the test area, 500 microseconds was used for the pulse delay.

When the projectile reached the second Kistler transducer another pulse was initiated that was relayed to a Kistler model 504A charge amplifier then to a Hewlett Packard Model 214A pulse generator. The pulse generator provided the voltage necessary to trigger the Pockel cell of the Korad K-1 pulsed ruby laser. This unit allowed for a variable signal delay which was used to adjust the time interval for laser firing. Two Monsanto Model 101B timers were incorporated into the system at various locations to provide checks on intervals of interest. Also a Korad KD energy monitor was employed to check the actual laser firing interval.

After firing, the test cell was closed and the hologram removed for processing. The armor plate was inspected for integrity and repositioned if necessary. The 20mm cannon was unloaded and the windows removed and examined for damage.

V. HOLOGRAPHIC FILM AND PROCESSING TECHNIQUE

The Korad K-1 pulsed ruby laser delivered a beam at a wavelength of 6943 \AA . In order to minimize the effects of extraneous light leakage into the system a photographic emulsion with narrow band sensitivity centered in this region was selected. Agfa-Gevaert 10E75 holographic plates were found to be the most suitable for this purpose. This film has a resolution capability of 2800 lines per mm. For holograms produced with 6943 \AA light this is nearly the required maximum resolution. Reference 4 gives a spectral sensitivity curve for the emulsion.

Following exposure to the laser light the hologram plate was removed from its holder and placed in a closed container and taken to a dark room for development. The initial processing required a five minute bath in kodak D-19 developer. The entire five minute bath was completed in total darkness. Then the plate was rinsed and placed for five minutes in a standard fixer. After 30 seconds in the fixer it was permissible, although not necessary, to turn on green photographic lights in the dark room. From the fixer the plate was washed in water for five minutes and then allowed to air dry. During the entire development

procedure, when it became necessary to touch the hologram it was handled by the edges in an attempt to keep the hologram clear of unwanted finger markings.

When using the 20-nanosecond ruby pulse, it was not possible to control exposure time. Therefore, to ensure the desired intensity, a combination of suitable neutral density filters were placed in the beam paths.

VI. RECONSTRUCTION

To reconstruct the holograms a 15-milliwatt Spectra Physics continuous wave, helium-neon laser was used for the reconstructing wave. A Spectra Physics collimator was fastened to the laser, causing the beam to be expanded to approximately four inches in diameter. The beam was directed to pass through the hologram as outlined in Part I. The converging real image was then photographed with a single reflex polaroid camera using type 55 positive-negative film. This film has a resolution capability of 150-165 lines per mm negative, 14-17 lines per mm positive, thus providing excellent results. The reconstruction process is illustrated in Figure 14. The negatives were further processed at the Naval Postgraduate School photo lab, from which prints were produced.

VII. COMPUTER PROGRAM FOR PREDICTIONS OF FLOW PARAMETERS

The computer program used to predict the velocity of the projectile, pressure and total energy of the flow field was an adaption of a program developed at the Naval Ordnance Laboratory. The program was originally concerned with the analysis of hypervelocity model launchers (Ref. 5). The method of analysis used was essentially a one-dimensional, Lagrangian scheme where the field was divided into six regions each of which in turn was divided into zones. At the interface of each zone mass points were inserted. Each mass was considered to consist of one-half of the mass of the adjacent zone. The hydrodynamic equations, in finite difference form, were then applied to each mass point during the particular interval of interest. The method employed was the "q" method of Von-Neumann and Richtmyer (Ref. 6 and 7).

The following equations were used for this method:

Isentropic flow energy equation;

$$\frac{\partial E}{\partial t} = -(P+q) \frac{\partial v}{\partial t}$$

Equation of motion;

$$\frac{\partial u}{\partial t} = - \frac{\partial (P+q)}{\partial x} \quad \frac{1}{M} A(x)$$

Equation of state;

$$P = P(E, v)$$

$$M = \int_0^X (X) A(X) dx$$

with $\left\{ \begin{array}{ll} \frac{C_0^2}{v} \frac{\partial u}{\partial y} & , \frac{\partial u}{\partial y} < 0 \\ 0 & , \frac{\partial u}{\partial y} \geq 0 \end{array} \right.$

The artificial viscosity term "q" was added to the pressure term in the energy and motion equations in order to spread variable changes created by the shock over a finite region. This allows the equation variables to be considered continuous across the shock. The constant C_0 permits adjustment of the shock "thickness."

The equations were written in finite difference form with initial values of E_0 , P_0 , and V_0 being provided for each region. In order to maintain stability during the process, a new time increment was calculated for each cycle.

During each cycle the pressure was calculated at each mass point using the equation of state and energy. The differential in pressure between mass points was then applied to the equation of motion to determine the acceleration and velocity of each mass point.

For each region it is necessary to input the initial temperature, pressure, molecular weight and a geometrical description.

The program was written in FORTRAN. A listing of the program and the input is given in Appendix A.

VIII. HOLOGRAPHIC RESULTS

Initially the first few holograms obtained appeared to be in the region several centimeters in front of the projectile. However, when further experimental studies did not give the desired results, an investigation was initiated to examine the laser system. It was then discovered that a short circuit had occurred between the plate and cathode of the large thyratron of the Korad power supply. This short circuit would occur approximately 8 minutes following the application of power. This malfunction caused a firing pulse to be continually delivered to the Pockel cell; thus, nearly two-thirds of the seventy-five test firings resulted in holograms in which the laser had fired from 50 to 200 microseconds early. To further compound the problem the Korad KD energy monitor was not available to confirm actual laser firing.

With the incorporation of the energy monitor into the system, and careful monitoring of the power supply, several good holograms were obtained. Figure 15 shows a series of compression waves approximately 2 cm in front of the projectile. Figure 16 shows these same type of waves

approximately 1 cm in front of the projectile. A traveling bow wave can be seen in Figure 17. It is believed that this wave is approximately 3 mm in front of the projectile.

Due to time consideration allowed for this study, the area just behind the projectile was not captured; however, Figure 18 shows a hologram obtained approximately 30 microseconds following projectile passage through the test area. The effects of powder blast not only etch the plexiglass windows but also leave a carbon deposit over the inner faces, resulting in a clouded view of the test area. Further investigations will determine if this powder blast is directly behind the projectile or if there are several microseconds delay between the gas particles and the projectile.

IX. COMPARISON OF ANALYTICAL AND EXPERIMENTAL RESULTS

Analytical results were obtained previously by Robert G. Bettinger (Reference 8) during his work concerning gas core characteristics in the muzzle environment of the 20mm cannon.

Figures 19 and 20 are outputs obtained by Bettinger. Figure 19 summarizes the major input data and initial conditions required, and demonstrates the output format used for representing these data. As shown in Figure 19, a printout was obtained every 0.2 milliseconds. Figure 20 illustrates the output obtained just as the projectile exits the barrel; at this time a muzzle velocity of 1064 meters per second was obtained.

It must be emphasized that the program (Reference 5) does not take into consideration the effects of frictional forces on the projectile. Therefore, in order to obtain a more realistic solution either the program must be modified or the powder parameters altered to account for this constraint. Figures 19 and 20 resulted from the latter choice.

In order to verify these results it was necessary to analyze the powder used to propel the 20mm projectile.

The type powder used in the 20mm cartridge was WC870 with a charge weight of 590 grains. WC870 is a sphere of .305" average grain diameter, with a specific gravity of 1.56 grams/cc. A representative composite is:

Nitrocellulose (13.15%N)	=	81.49%
Nitroglycerine	=	10.0 %
Dibutylphthalate	=	5.5 %
Diphenylamine	=	1.0 %
CaCO ₃	=	0.1 %
AsH	=	0.5 %
Graphite	=	0.15%
Na ₂ SO ₄	=	0.16%
K ₂ SO ₄	=	0.75%
SNO ₂	=	0.75%
Ethyl Acetate	=	0.10%
H ₂ O	=	0.80%

The percentages are given of the dry weight, so that the sum of the ingredients up to the last two constituents is 100%.

The average thermochemical properties of this composition are (by Hirschfelder's approximation, reference 1) as follows:

T ₀	=	2856°K
n	=	0.04218 grams/mol
χ	=	1.2394
F	=	335068 ft-lbs/md
b	=	0.943 cc/gram

The molecular weight of the constituents can be found directly except for nitrocellulose. The nitrocellulose in propellant compositions varies in its nitrogen content. The cellulose molecule is a large one but, for present

purposes, it can be written $C_6H_7O_2(OH)_3$. On nitration, $X(OH)$ groups are replaced by (ONO_2) groups, the value of X depending on the nitrogen content. The resulting compound is $C_6H_7O_2(OH)_{3-X}(ONO_2)_X$. The molecular weight is easily found to be $(162.14 + 45X)$ and, if Y is the percentage nitrogen content, $Y = \frac{1400.8X}{162.14 + 45X}$. This gives $X = \frac{162.14Y}{1400.8 - 45Y}$. Thus for a given nitrogen content Y and X can be calculated and the atomic composition found from:

$$C = \frac{6}{162.14 + 45X} \quad H = \frac{10-X}{162.14 + 45X} \quad N = \frac{Y}{1400.8} \quad O = \frac{5 + 2X}{162.14 + 45X}$$

The heats of formation of the solid propellant can be calculated as outlined in Reference 10.

Inputting the exact values into the computer program resulted in a value of approximately 1463 M/sec. Assuming a projectile drag coefficient of 0.28 (Reference 9), this gives a muzzle velocity of 1036 meters per second which is in excellent agreement with Bettinger's theoretical results.

Furthermore, the maximum possible muzzle velocity (Reference 1) may be calculated from the following:

$$V_m = \frac{2}{\gamma - 1} (RT_0)^{\frac{1}{2}}$$

Using this equation a value of 1097 meters per second is

obtained. The projectile velocity was measured during each firing, and a range of 1020 to 1060 meters per second was obtained.

These values are in excellent agreement with the computer program.

X. SUMMARY AND RECOMMENDATIONS

A considerable amount of difficulty was experienced while attempting to capture the projectile in the test area. Considering the velocity and length of the projectile, passage through the test area occurs within approximately 80 microseconds. Furthermore, considering just the base of the projectile, a time interval of approximately 20 microseconds would result in complete passage of the base of the projectile through the test area. Thus, timing of the laser firing with projectile firing is indeed quite critical.

Referring to Figure 21, it can be seen that the velocity of the projectile approaches a constant value at a distance of approximately 90 cm from the breech of the barrel. It was this fact that prompted the barrel modification to incorporate the pressure transducer near the test area as outlined in Part III Section B. By controlling the firing of the Pockel cell with this transducer, more consistent results were expected.

Theoretically, if the pressure transducer responded instantaneously to the passage of the gas ring of the projectile, the signal produced could be used to pulse the

Pockel cell of the laser just as the nose of the projectile entered the test area.

Unfortunately, 0.5 volts was required to trigger the Hewlett Packard Model 214A pulse generator, while the Monsanto timers responded immediately to projectile passage. Referring to the pressure trace obtained from the pressure transducer (Figure 22), approximately 100 microseconds could pass before the required 0.5 volts was obtained.

In an attempt to confirm the actual passage of the projectile through the test area the pressure transducer was replaced by a temporary contact switch. This switch could only be triggered by actual contact with the gas ring of the projectile. The test confirmed the correct timing of the projectile, agreeing with the results obtained with the pressure transducer as far as the Monsanto timers were concerned.

Due to the fact that most pulse generators require at least 0.5 volts input as a trigger and that the pressure transducer used takes anywhere from 0-100 microseconds to reach 0.5 volts, it is felt that a more positive device must be used to sense the actual position of the projectile. This could be accomplished with a contact switch designed specifically for this purpose.

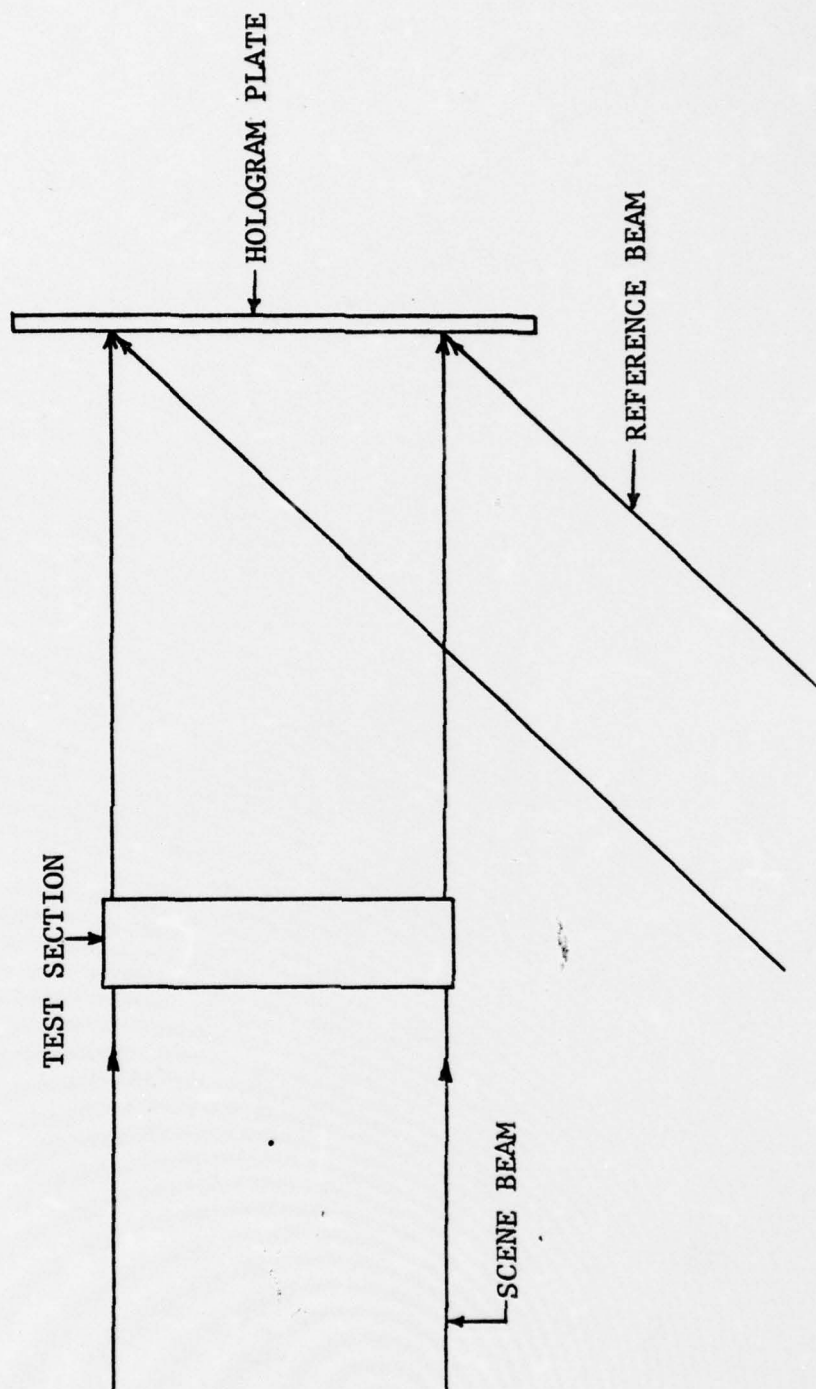
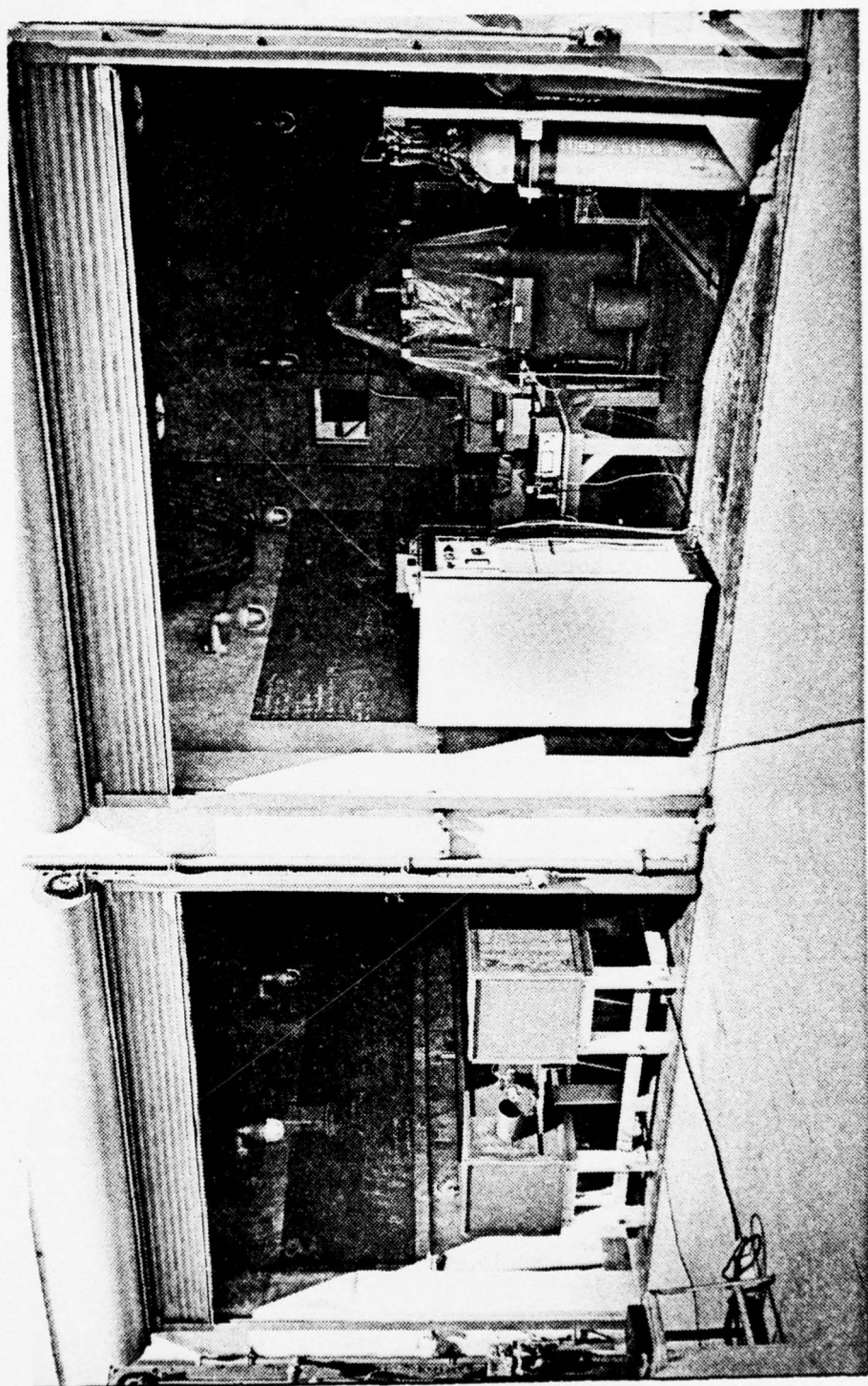


Figure 1. Direct Illumination Method of Obtaining a Hologram

Figure 2

Laser Installation

Cannon and Optics Cell



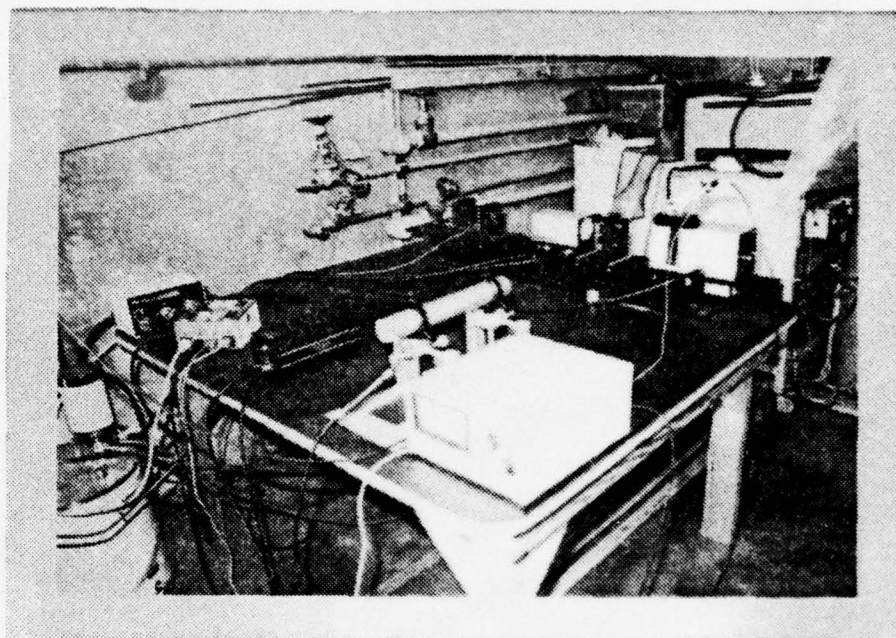


Figure 3. Laser Setup

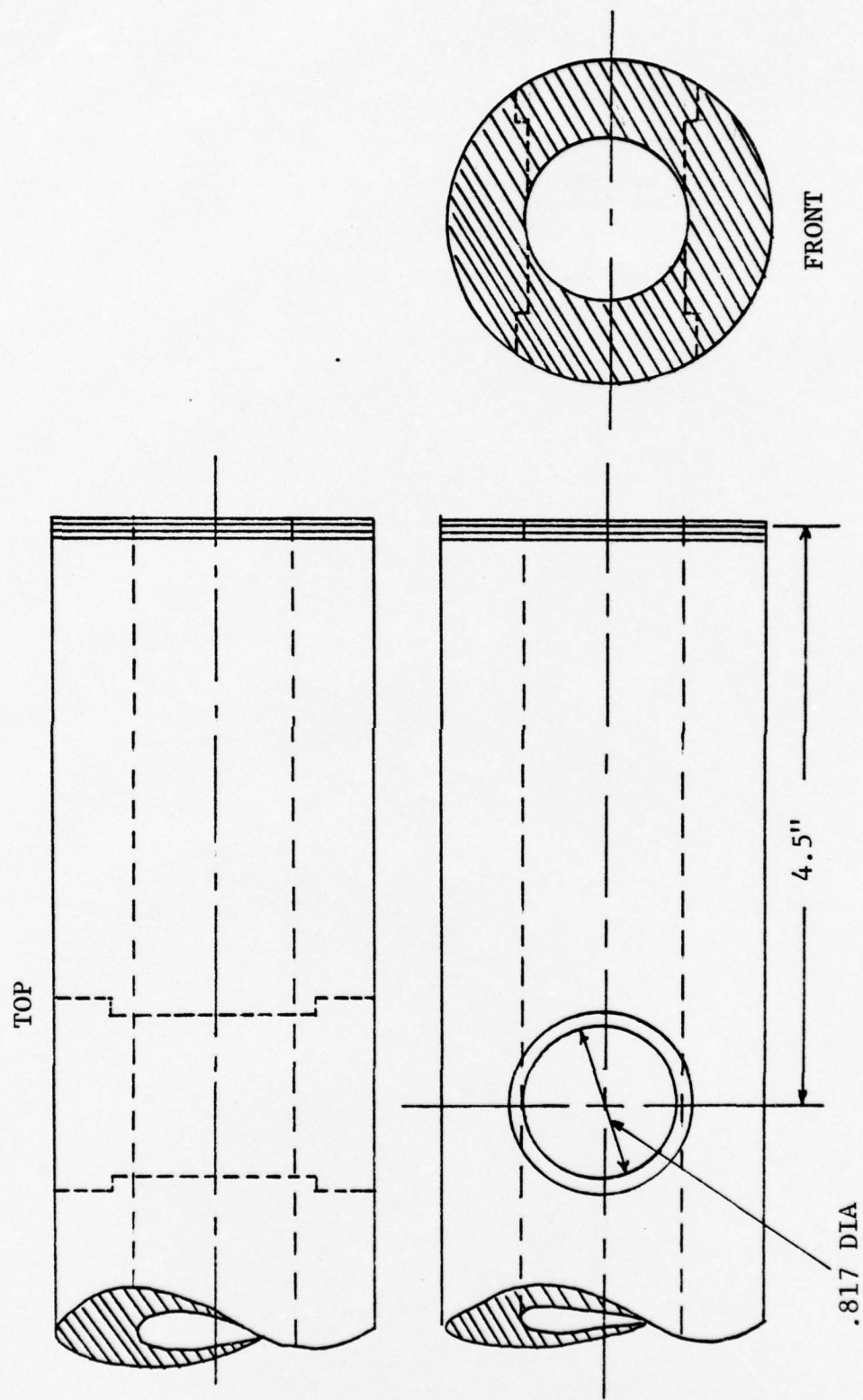
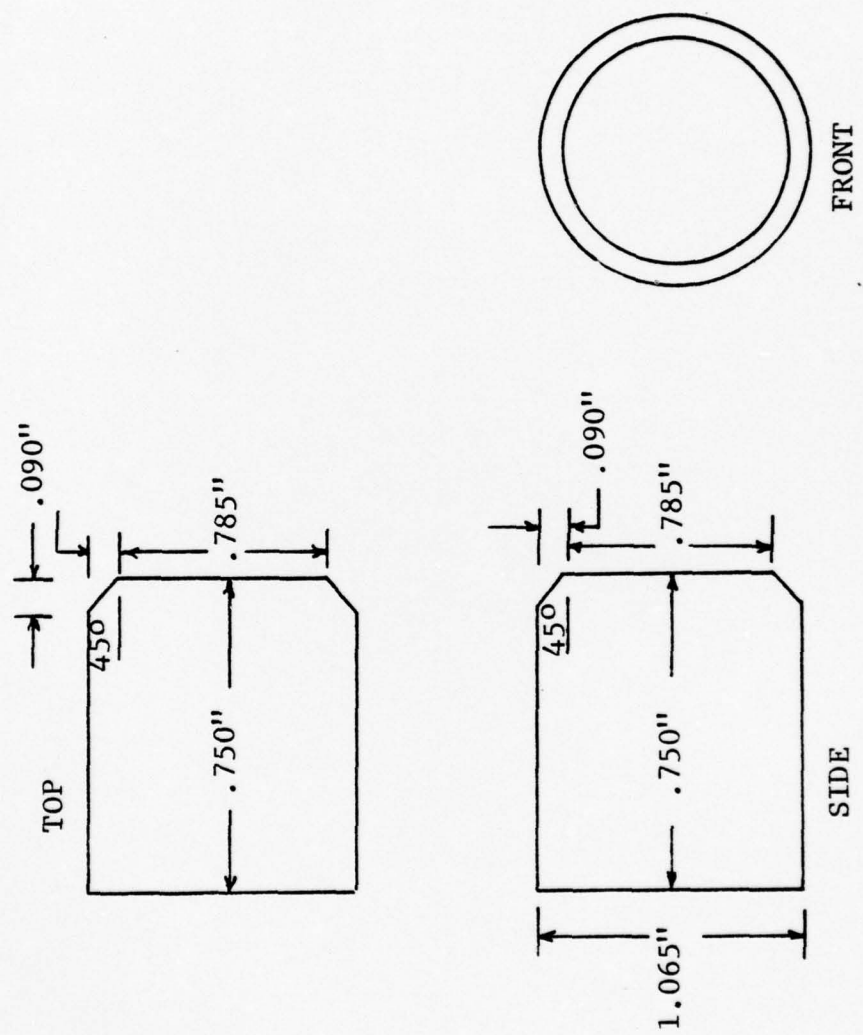


Figure 4. Barrel Design



NOTE: Windows to be seated with #118 O-ring

Figure 5. Plexiglass Windows

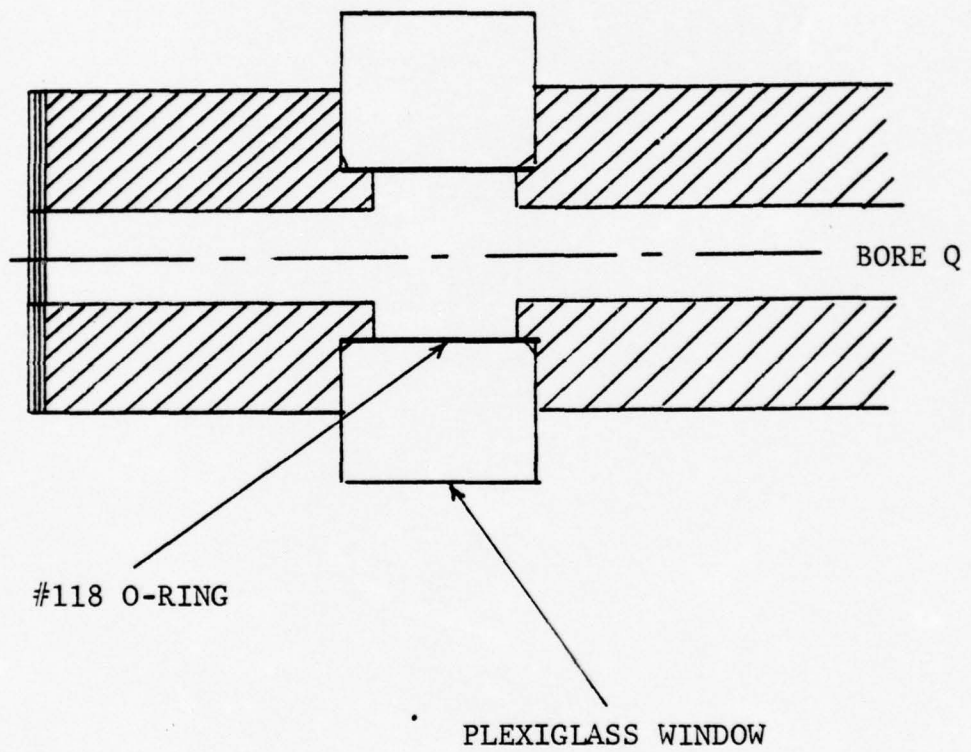


Figure 6.
Top Cutaway View of Barrel with
Plexiglass Window Installation

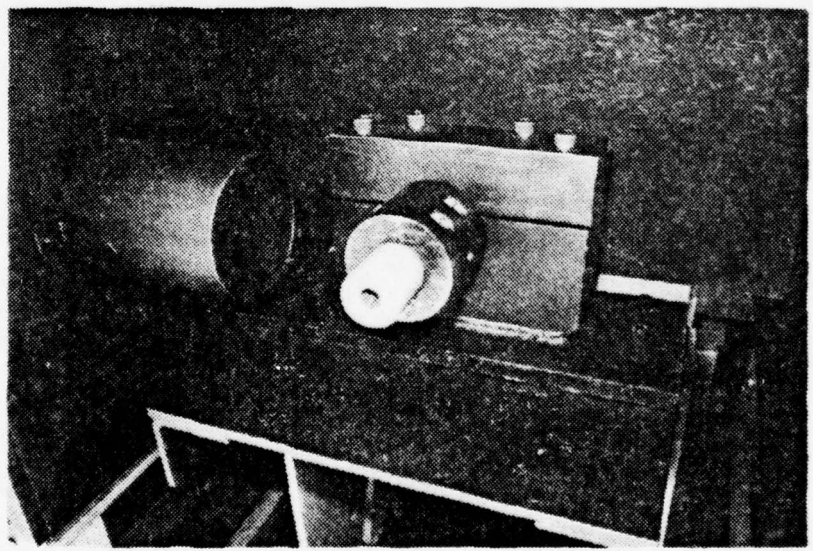
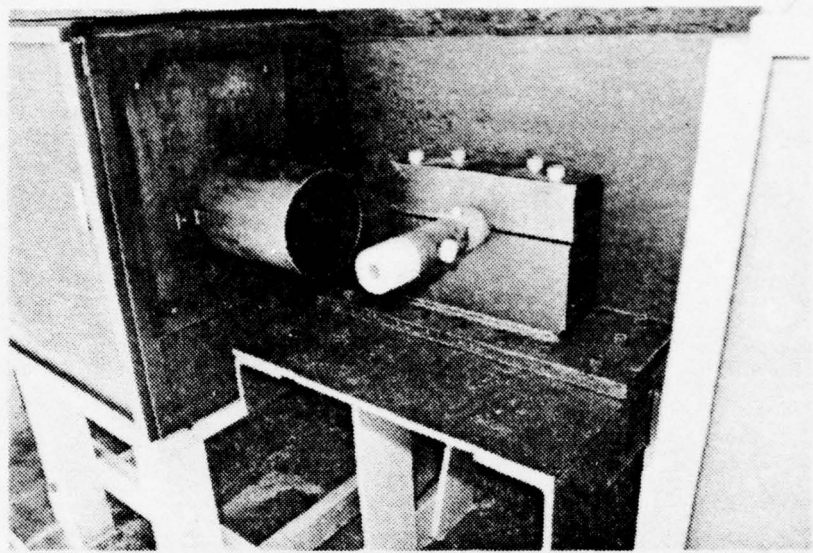


Figure 7. Barrel with Windows and with Collar

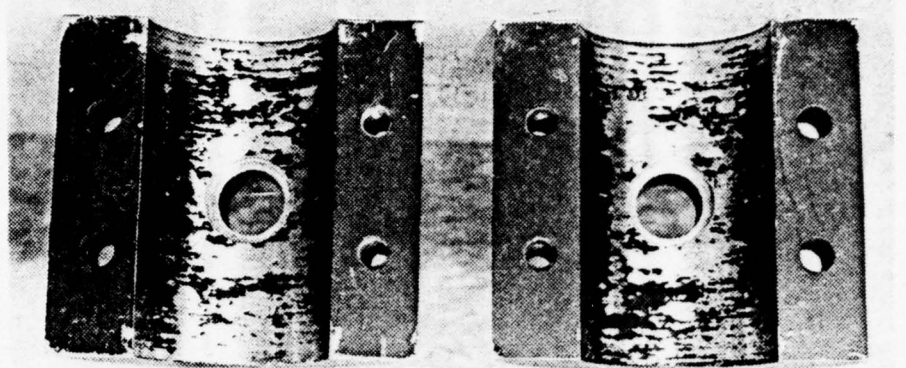


Figure 8. Collar Device



Figure 9. Projectile Path and Turret with Velocity Screen in Place

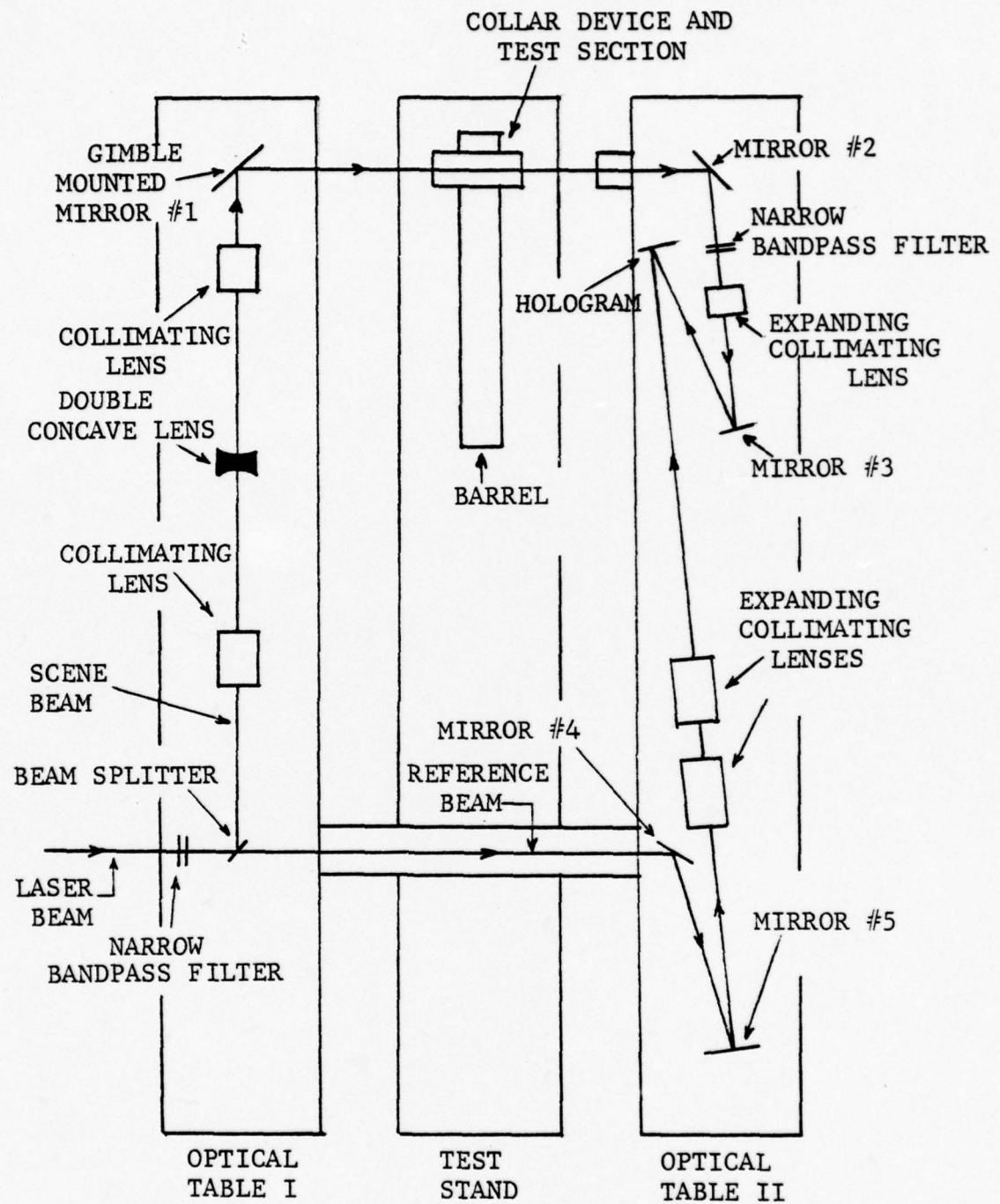


Figure 10. Optical Arrangement

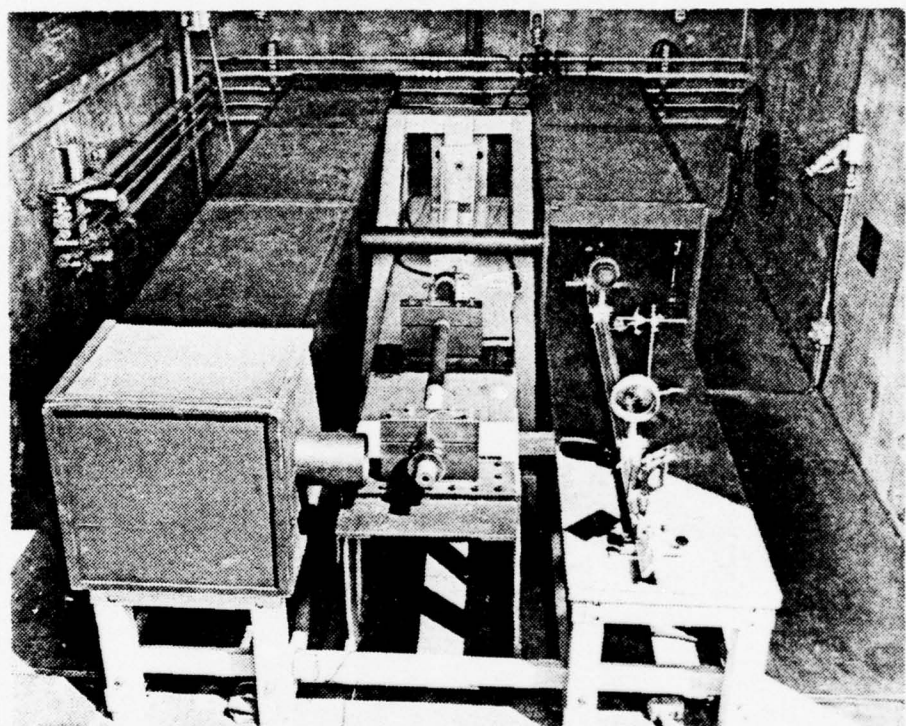


Figure 11. 20mm Cannon with Optical Platform

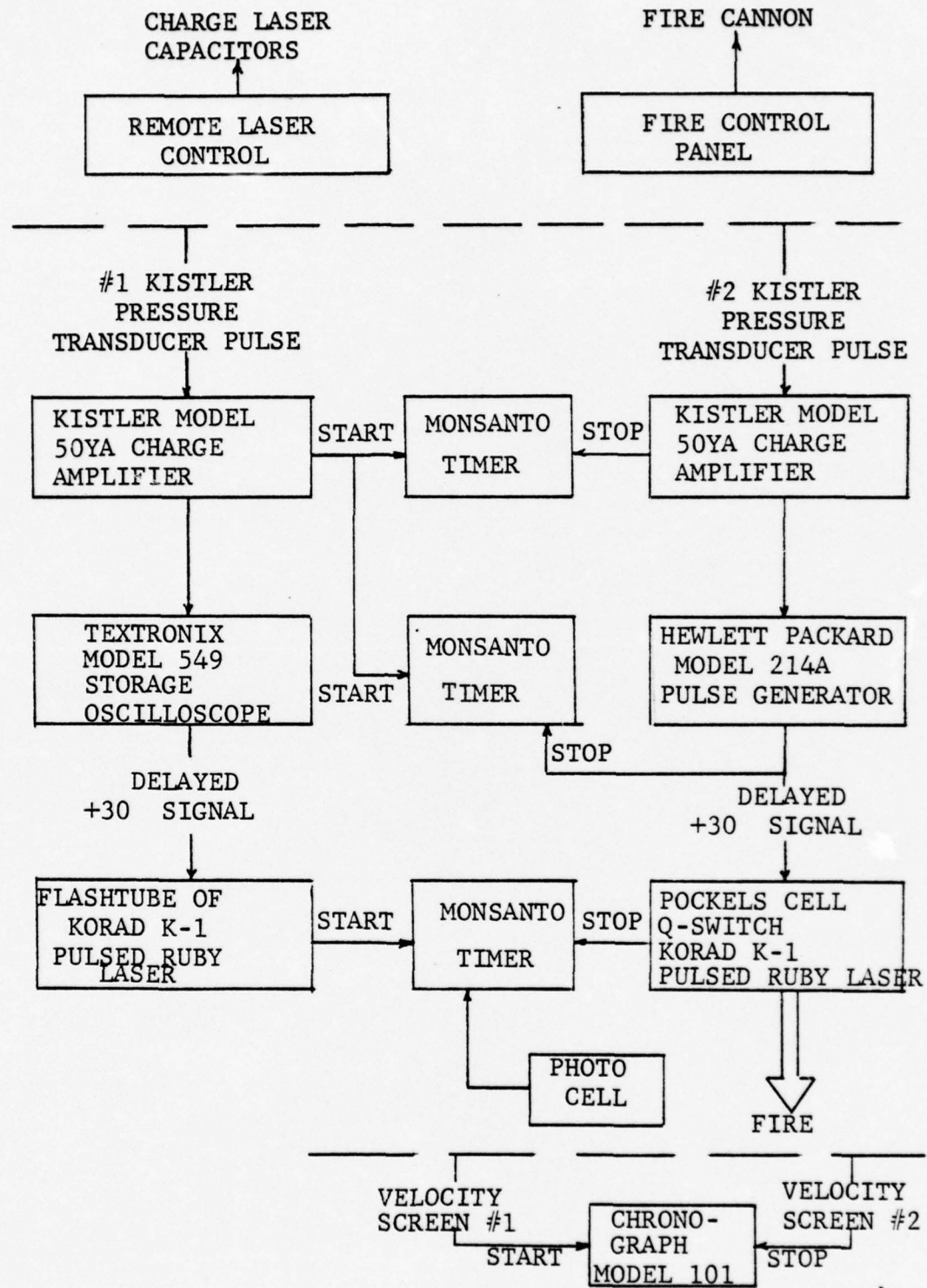


Figure 12. Firing Sequence

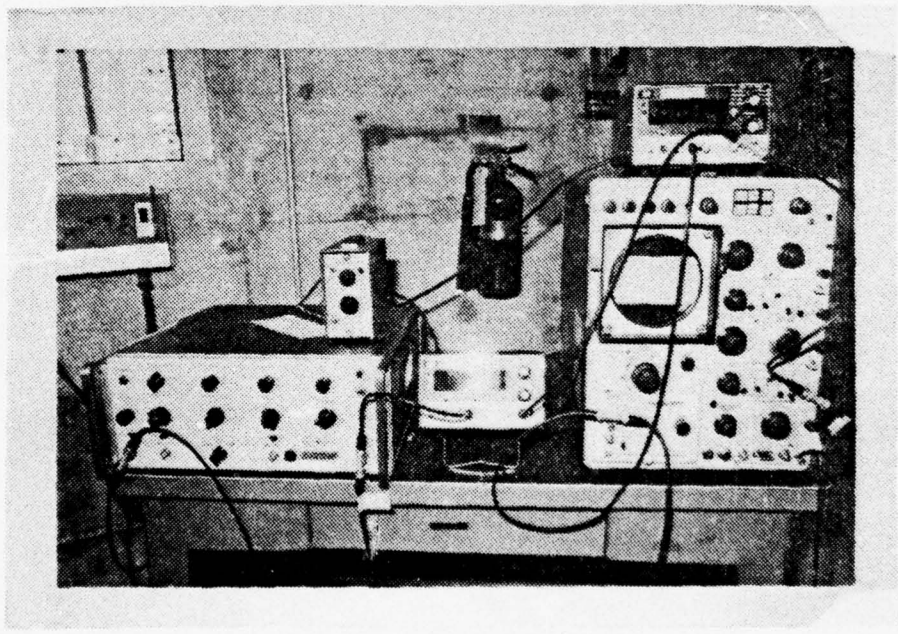
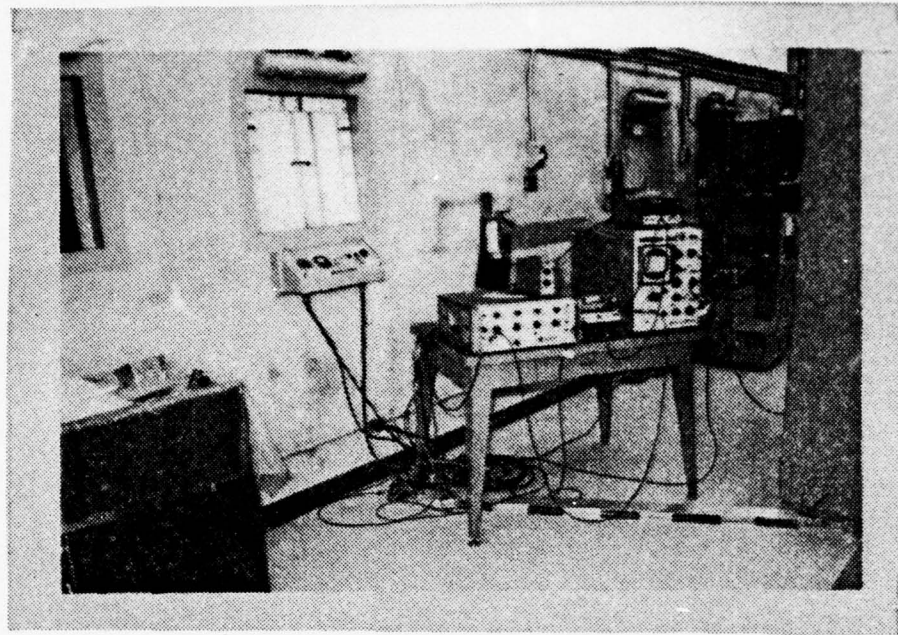


Figure 13. Control Room and Monitoring Equipment

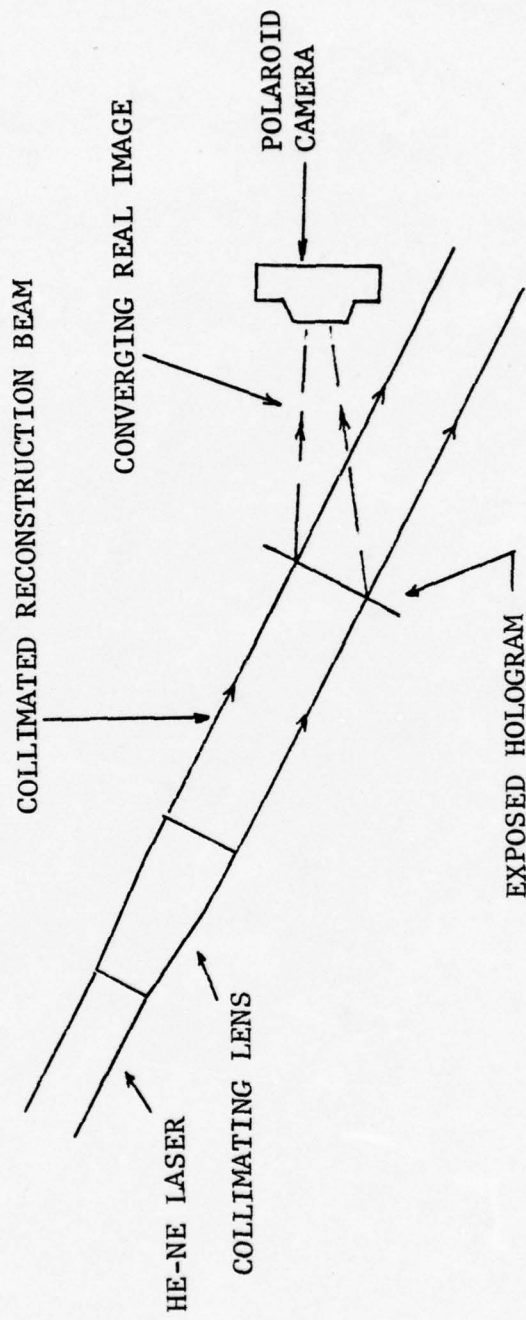


Figure 14. Reconstruction

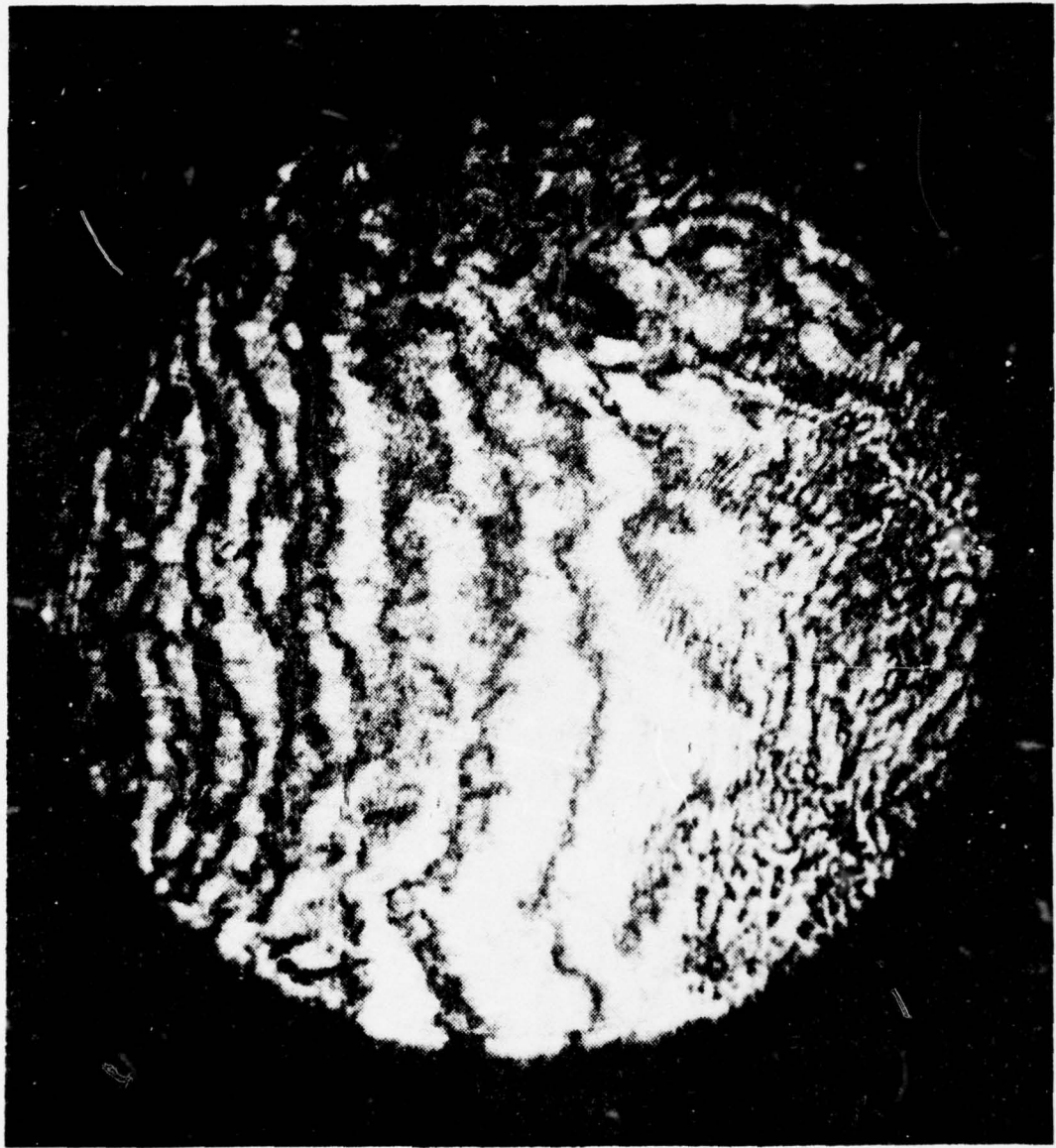


Figure 15. Compression Waves

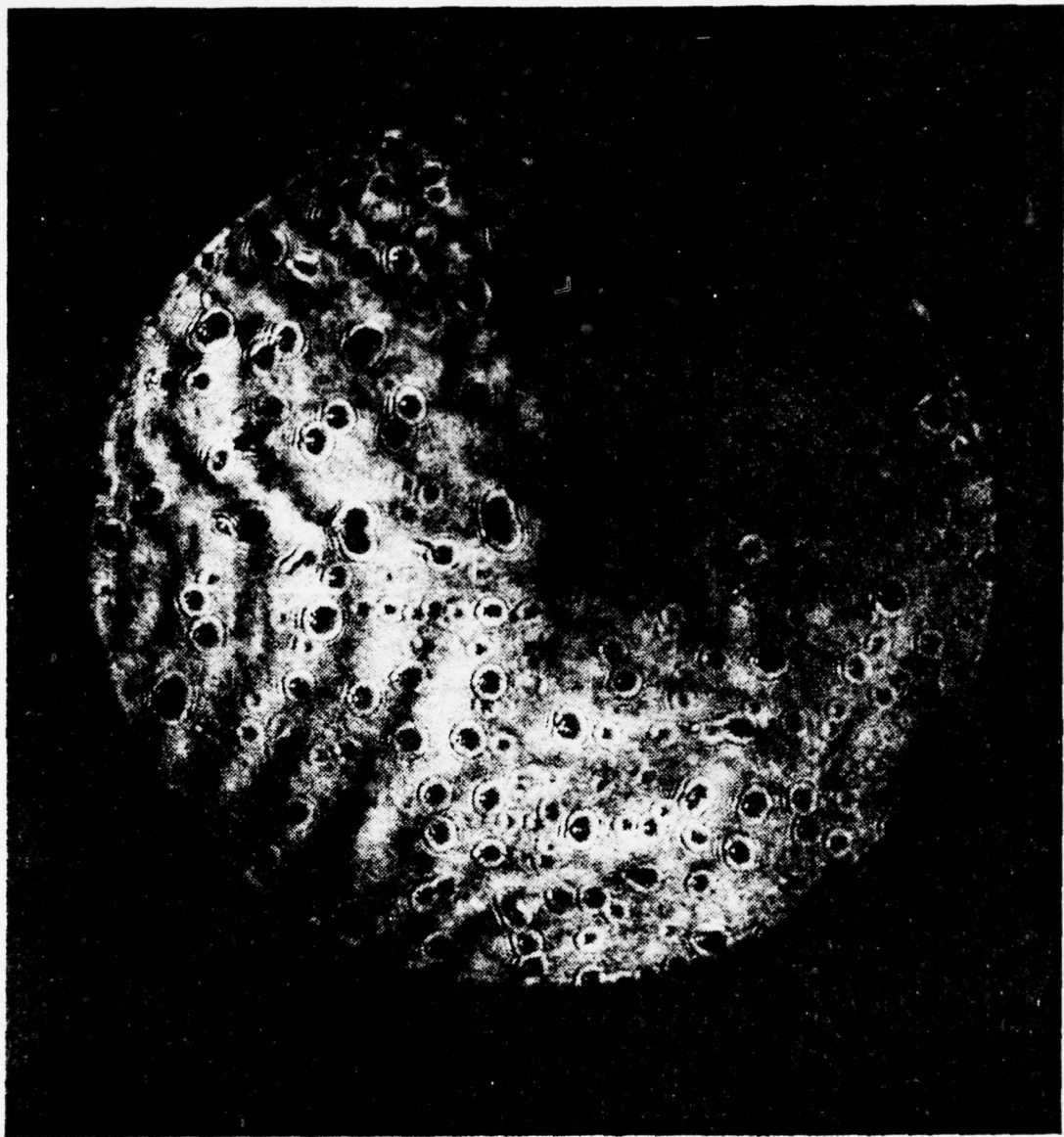


Figure 16. Compression Waves

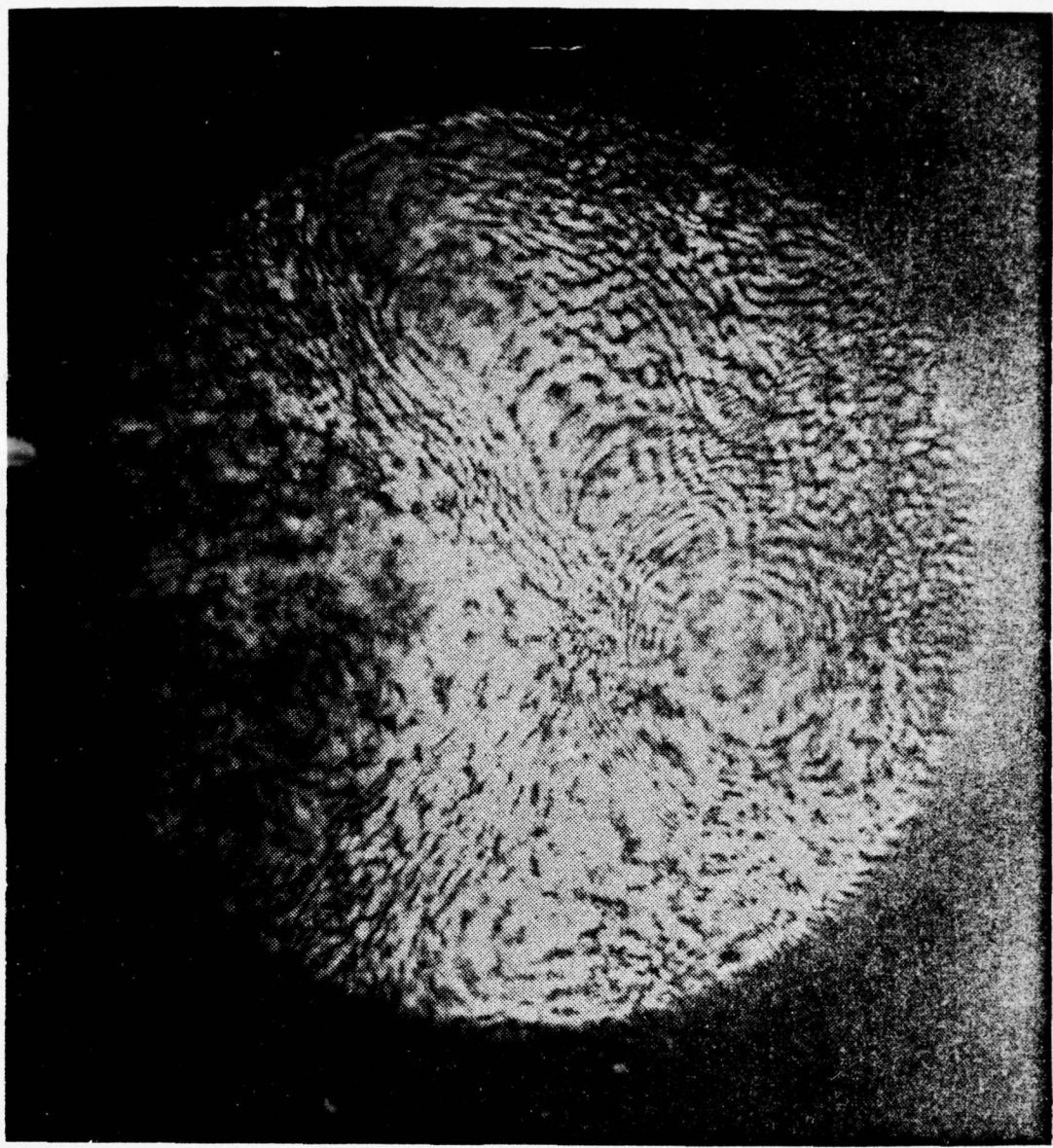


Figure 17. Bow Wave



Figure 18. Hologram Showing Carbon Deposits

GUN BARREL PROJECT

Demensions: 6 Regions, 6 Zones

<u>Regions</u>	<u>Zones</u>	<u>Length (cm)</u>	<u>Area (cmsq)</u>	<u>Volume (cc)</u>
1	1	1.47	2.95	4.35
2	1	1.47	2.95	4.35
3	1	1.47	2.95	4.35
4	1	1.47	2.95	4.35
5	1	1.47	2.95	4.35
6	1	5.40	2.95	15.93

INITIAL CONDITIONS

Powder Conditions: Grams Powder = 38.23
TBURND = 1.00 Millisec

Materials:

<u>Region</u>	<u>NEQST</u>	<u>Pressure (psi)</u>	<u>Temp. (Deg. K)</u>	<u>Molec. Wt. (gm/mole)</u>
1	2	14.7	300.0	125.00
2	2	14.7	300.0	125.00
3	2	14.7	300.0	125.00
4	2	14.7	300.0	125.00
5	2	14.7	300.0	125.00
6	3	3.0	300.0	55.85

Print out every 0.20 millisec up to 10.00 millisec

Print out every 0.050 millisec up to break

Print out every 0.200 millisec up to launch

Mass of Projectile = 90.0 gm

Break Valve Strength = 690.0 Bars

Number of Pressure Points: 1

Location of Pressure Points: 14.0 cm

Figure 19. Computer Output Format

GUN BARREL PROJECT

Cycle 290 T(Millisec) 1.88443E00
 DT(Millisec) 2.18257E-02

j	X(CM)	VELOCITY (CM/MS)	PRESSURE (BARS)
1	0.0	0.0	1.01381E 03
2	1.46490E 02	1.01004E 02	8.52849E 02
3	1.47602E 02	1.03653E 02	7.78181E 02
4	1.48734E 02	1.06449E 02	8.85098E 02
5	1.49668E 02	1.07232E 02	1.05442E 03
6	1.50551E 02	1.06399E 02	3.98267E 02

Figure 20. Computer Output Format

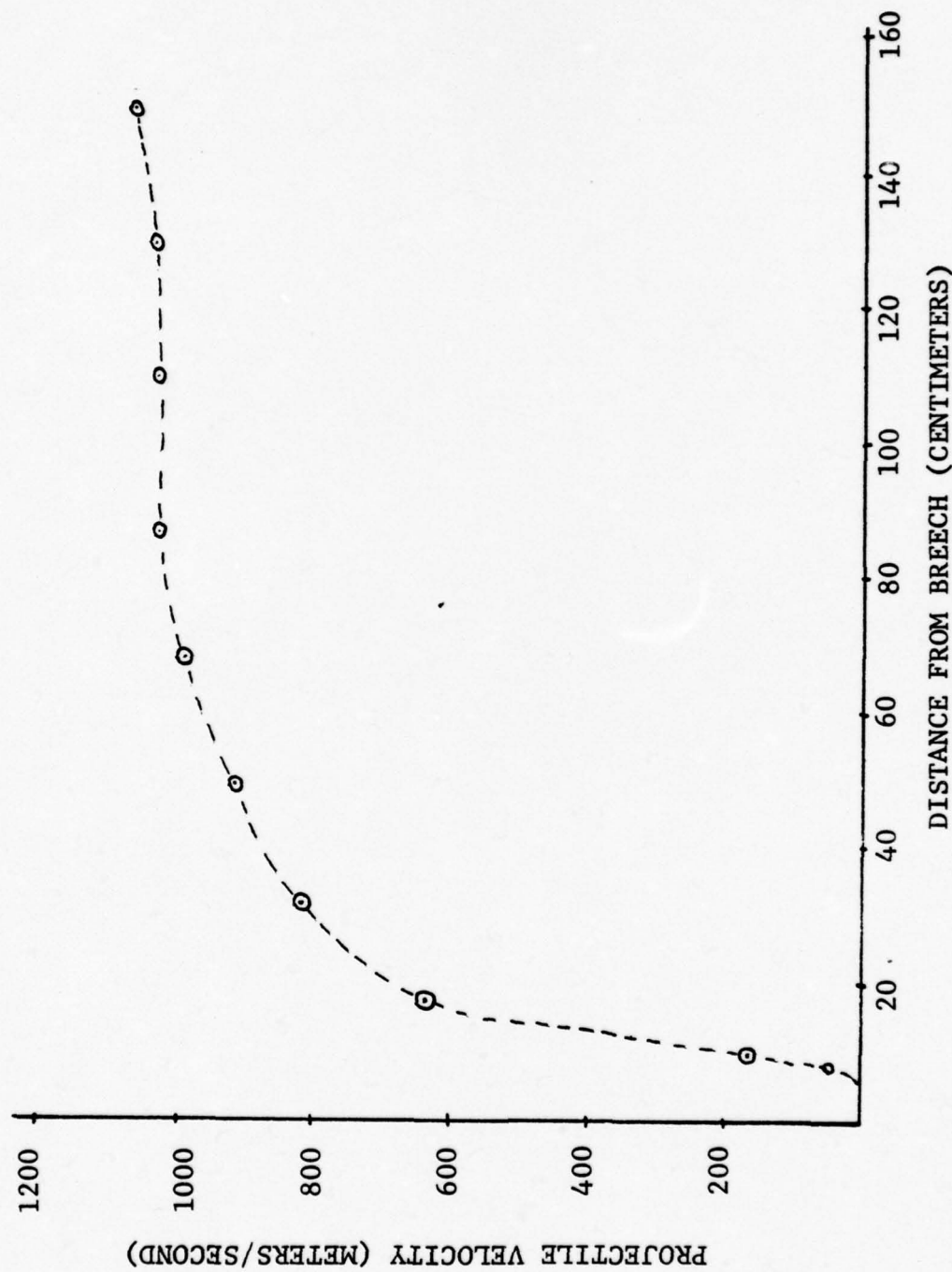


Figure 21. Projectile Velocity vs. Position

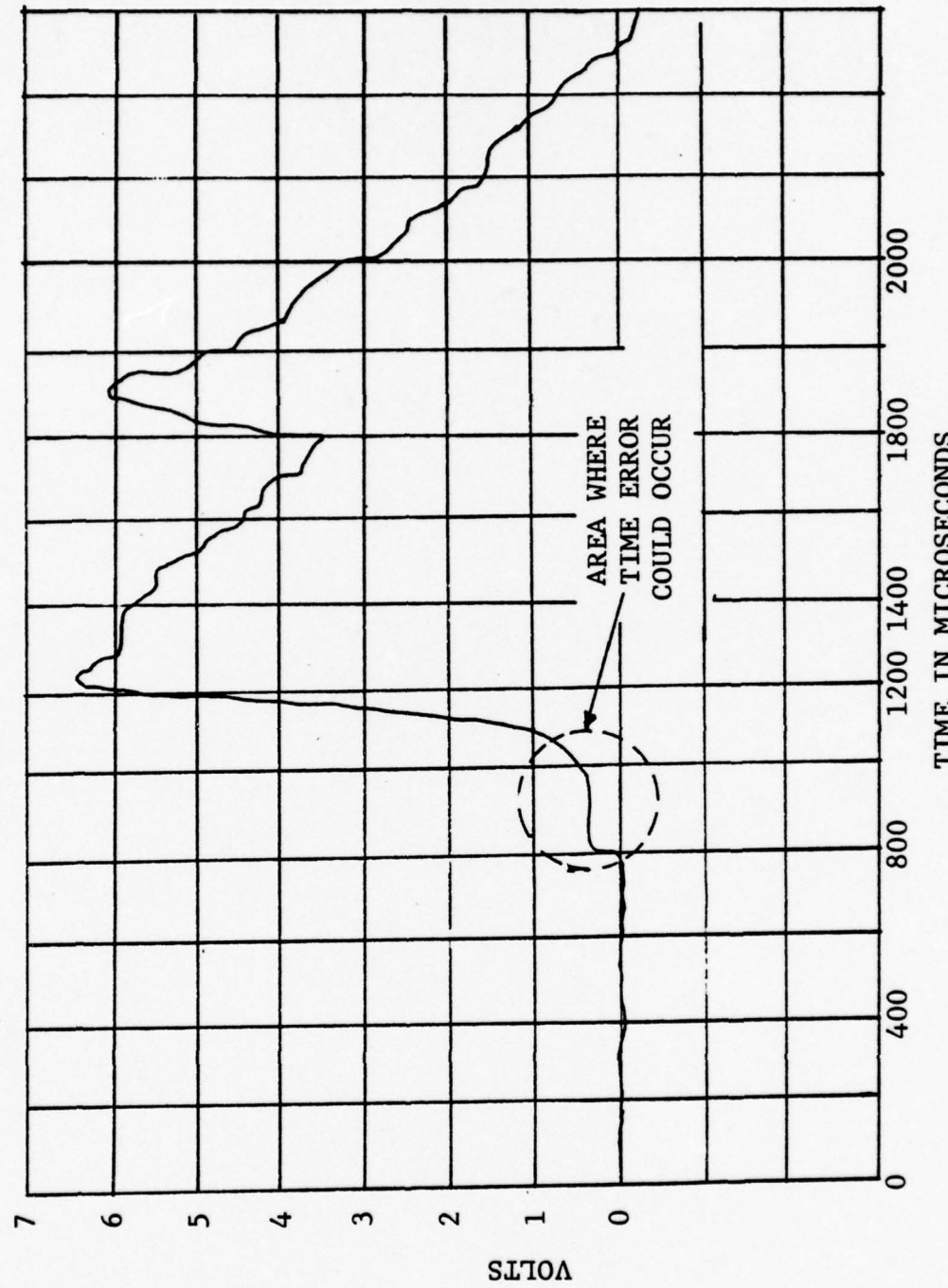


Figure 22. Pressure Trace Output from Pressure Transducer
Locate 2.5 inches Aft of Observation Port

APPENDIX A
GUN PROJECT

6

```

T=0.0
I=DATA NREAD,NPRINT/5,6/
M=6
NI=0
NPVITR=1
1 CALL ZEROAB(500,XP1,XP2,PP1,VP2,XP3)
CALL ZEROA(500,PP3,PP1,PP1,PP1)
INTERJ(31)=M
CPMAX=0.0
PTMAX=0.0
ANFMAX=0.0
N1IMPT=0
IP=0
INFUNC=1
IPUNCHX=0
LN=0
IPV1=1
IPV2=2
C INC INITIAL CONDITIONS FOR PROGRAM, BEGIN INPUT FOR RUN, NEW OR IT
IF(NPVITR.EQ.1) GO TO 41
NPVITR=1
C INPUT FOR ITERATION FROM STORAGE
CALL STORE(ISTORM,STORM)
EMLEAD=STORM(97)
HYCRD1=STORM(98)
HYCRD2=STORM(99)
NEQST(30)=ISTORM(100)
IF(I DATA) 8,8,608
41 CONTINUE
INPUT FOR NEW RUN STORAGE OF INPUT
READ(NREAD,604) I DATA,IPRNTZ,ITRNSF,IPUNCH,DTSQ(199)
604 FCFMAT(413,F10.0)
IF(ITRNSF.EQ.0) GO TO 619
M=6
INTERJ(31)=M
619 IF(I DATA) 606,606,620
608 READ(NREAD,READD)
GO TO 610
C CALL READ
READ(NREAD,20) IPOX1,NPOX1(XPO(M),M=1,NPOX)
6 READ(NREAD,49) XPV1,PVERR,EMLEAD
READ(NREAD,6) EPIST,FRAC,EMLEAD
6 FORMAT(E10.4,3F10.0)
READ(NREAD,49) (AMOL(I),I=1,IMAX)

```

```

      READ (NREAD,49) (TO(I),I=1,IMAX)
      READ (NREAD,49) (PO(I),I=1,IMAX)
49   COUNTINUE
      CALL STORIN ('ISTORM, STORM')
      STORM(97)=EMLEAD
      STORM(98)=HYDRD1
      STORM(99)=HYDRD2
      STORM(100)=IPDX
      INITIAL CONDITIONS AND CONSTANTS FOR RUN
      INPT=NZONE(1)+NZONE(2)+NZONE(3)+1
      XSEGST=FRAC#OUTBDY(5)
      NEGST(30)=IPDX
      CALL CALCU(EMLEAD)
      IF(NI*NE*O)GO TO 603
      CALL PRINTO(EMLEAD,Frac,XPV1,XPV2,PVWANT,NPCX,IPCX,XPO)
      IF(IPRNTZ*EQ*0)GO TO 603
      READ(NREAD,11)LASTK
      IF(ILASTK)123,12,1
      CALL SETUP
      DO 706 IMP=1,ILAST
      PMODMIN(IMP)=PPLUSQ(IMP)
      PMODMAX(IMP)=PPLUSQ(IMP)
      MAIN LOOP OF PROGRAM - DYNMEQ, LFTOVER, AND OUTPUT
      603 CALL DYNMEQ
      706 CALL LFTOVER(IPNCHX)
      DO 710 IMP=1,ILAST
      IF(PPLUSQ(IMP)*GT*PMODMIN(IMP)) GO TO 705
      PMODMIN(IMP)=PPLUSQ(IMP)
      TNDMIN(IMP)=T
      IF(PPLUSQ(IMP)*LT*PMODMAX(IMP)) GO TO 710
      PMODMAX(IMP)=PPLUSQ(IMP)
      TNDMAX(IMP)=T
      710 COUNTINUE
      IF(IPUNCH*EQ*0*OR*JPROJ*NE*300) GO TO 627
      PRSTAB(NPUNCH+1)=T-DTSQ(200)
      NPUNCH+1
      JFLHAF=INTERJ(6)
      J=JPLHAF=JPLHAF-1
      JMNHAFF=JPLHAF-1
      DUD1=26*18*PPLUSQ(JMNHAFF)-1./9.*PPLUSQ(JMNHAFF-1)
      PRSTAB(NPNP1)=DUD1
      707 IF(STGT*(DTSQ(200)+DTSQ(199))=PRSTAB(NPNP1)) GO TO 647
      PRSTAB(NPNP1)=NPUNCH+2
      NPUNCH=NPUNCH+1
      IF(S1-NPUNCH)625,627
      PUNCH641=PRSTAB
      641 FORMAT(3(F12.8,E12.8))

```

```

NPUUNCH=1
CONTINUE
C
627 72 C CONTINUE OF MAXIMUM PRESSURES
      INTER51 = INTERJ(6) -1
      CPMAX = AMAX1(PMAX, PPLUSQ(NPTN-1))
      PPLUSQ(NPTN-1) PPLUSQ(NPTN-2), PPLUSQ(NPTN-3)
      AMPMAX = AMAX1(AMPMAX, PPLUSQ(INERS51))
      DETERMINATION IF MODEL HAS BEEN LAUNCHED
      IF(XSTOP-(JLAST*NPLUS1)) 9 TO 3
      IF(IPOX*EQ.5) GO TO 2
      IF((X(NPTN, NI).LT. XST) GO TO 1
      GO TO 2
      KN = NCYCLE/6
      KN = KN
      SN = SN/6
      STF((TN-QN)) 41 41^2
      GO TO 7
      LN = LN + 1
      IPOX*EQ.6) GO TO 75
      IF((IPOX*EQ.1) GO TO 51
      DO 60 INPOX=INPOX+1 NPOX
      IF((ISTOPX(INPOX).GE.1) GO TO 60
      NTIMPT=LN
      DC 58 INPTN=2, JLAST1
      IF((XPO((INPOX).LT.XI(INPTN)) GO TO 59
      58 CONTINUE
      DUMVAR(LN,INPOX)=PPLUSQ(INERS51)
      NPTPL(INPOX)=LN
      GO TO 60
      DUMVAR(LN,INPOX)=PPLUSQ(INPTN-1)
      NPTRL(INPOX)=LN
      59 1/(X1(INPTN-1)-XI(INPTN))*(XPO((INPOX)-X1(INPTN-1))-PPLUSQ(INPTN-1))
      IF((LN.EC.1099) GO TO 55
      GOTOP(X(INPOX)=2
      NPTRL(INPOX)=LN
      55 CONTINUE
      60 IF((IPOX*NE.6) GO TO 78
      75 DUMVAR(LN)=1 =PPLUSQ(INERS51)
      78 IF((IPOX.EQ.6) GO TO 2

```

```

C      51 IF(IPOX.EQ.2) GO TO 52 FIND MAX IN REGION TO GO HERE
C      52 CONTINUE OF MODEL PLOTS AFTER BREAK VALVE
C      7 IF(JPROJ=300) 13,513
      5 IF(IP.GT.498) 60,T0 2
      1 IF(XSTO.PEQ.3000.) GO TO 76
      10 XP1(IP)=X(JLAST,N)
      10 XP2(IP)=X(JLAST,N)
      PP1(IP)=P(PLUSQ,INER51)
      VP2(IP)=U(JLAST, NMNHAF)
      13 GO TO 2 OF RETURN TO MAIN LOOP OF PROGRAM, AND WRITING OF ALL PLOT TAGS
      13 FCINT OF FINAL STORAGE OF POINTS TO BE PLOTTED, AND WRITING OF ALL PLOT TAGS
      9 IF(IPOX.EQ.5) GO TO 25
      9 IF(IPOX.EQ.6) GO TO 76
      1 IP=IP+1
      1 XP1(IP)=X(JLAST,N)
      1 XP2(IP)=X(JLAST,N)
      PP1(IP)=P(PLUSQ,INER51)
      VP2(IP)=U(JLAST, NMNHAF)
      GU TO 36
      35 NPOX=1
      35 DO 70 IPLTXT=NPTPL(IP,TXT)
      35 NPTTX=NPTPL(IP,TXT)
      35 IF(NPTTX.NE.10) GO TO 70
      35 NPTTX=NPTPL(IP,TXT)
      35 DO 80 ITXP=1,NPTTT
      35 TPLT(ITXP)=TPOX(ITXP)
      35 PPLT(ITXP)=DUMVAR(ITXP, IPLTXT)
      35 IF(JPROJ.NE.300) GO TO 1
      70 CONTINUE
      76 DO 93 ITXP=1, LN
      93 PPLT(ITXP)=DUMVAR(ITXP,1)
      C      93 PPLT(ITXP)=DUMVAR(ITXP,1) FOR NEW INPUT
      25 READ(NREAD,11) ILASTK
      25 IF((IPUNCH.EQ.0).OR.(NPUNCH.EQ.1)) GO TO 629
      25 NPUNCH=NPUNCH-1
      629 CONTINUE
      629 WRITE(6,45) CPMAX, PTMAX, AMPMAX
      629 WRITE(6,704) ((IT, PMDMIN(IT), TMDMIN(IT)), TMDMAX(IT))
      1 IF(IT=1) JLASTK
      1 FORMAT(132X,E12.6,2X,E12.6,2X,E12.6)
      704 FORMAT(3F20.2)
      45 IF(ILASTK) 15, 12, 1

```



```

      READ(1,NREAD,5)CALPGM,TBURND,GMS PDR,GASPRS,IHEL
      READ(1,NREAD,5)HYDRD1,HYDRD2
      FORMAT(2E15.5)
      WRITE(6,123)HYDRD1,HYDRD2
      123 FORMAT(4F10.0)14)
      5 FORMAT(7F10.0)
      100 RETURN
      903

```


6


```

5SKIN(200),TSIGSQ(200),TMINSQ(200),TOVRE1(30),THETA(200),UZERO(30),
6UASS(200),VS(200),VZER(30),V(30),VSCOS(200),X(200),X(200),X(200),
7ZLAST=DTMIN(NPLHAF),
N=INTERJ(31),
SIGMAX=EQ(0) GO TO 240
SIGMIN=1.0/SIGMAX
SIGTO=24
SIGMIN=0.0
244 IF(SIGMIN-7.41*TMINSQ(NPLHAF)) 270,270,250
250 IF(DLAMAX-1.11*TMINSQ(NPLHAF)) 270,270,260
255 IF(SIGMIN-1.11*TMINSQ(NPLHAF)) 265,260,260
260 IF(DLAMAX-0.65*TMINSQ(NPLHAF)) 270,270,265
265 IF(INSQ(NPL3HF)=TMINSQ(NPLHAF)
285 GC TO 285
270 IF(DLAMAX-0.01)=SIGMIN/2.25
275 GC TO 285
280 TMINSQ(NPL3HF)=AMIN1(SIGMIN/9.00*005184*TMINSQ(NPLHAF)/DLAMAX**2)
285 DTMIN(NPL3HF)=AMIN1(SQR(TMINSQ(NPL3HF)),1.4*DTMIN(NPLHAF))
290 DTWIN(NN)=(DTMIN(NPL3HF)+DTWIN(NPLHAF))/2.
NPLUS1=NPLUS1
NPLHAF=NPLUS1
N=NP
NMHAF=N
NPL3HF=N
EINSUM=0.
EKSUM=0.
DO 300 I=1,IMAX
  DO 301 J=0,
    EKIN(I)=INTERJ(I+1)-1
    JMAX=INTERJ(I)
    DO 295 J=JMIN,JMAX
      JPLHAF=J
      JSQ(J+1)=U(J+1,N)**2
      X1-JPLHAF=EINT(I)
      EKIN(I)=EINT(I)+(X1-JPLHAF)/HALFRO(I)*HALFM(JPLHAF)
      EKIN(I)=5*EKIN(I)
      EKIN(I)=EINSUM-EINT(I)
      EKIN(6)=5*EMPROJ*(JLAST,NMNHAF)**2+EKIN(6)
      EKSUM=EKSUM+EKIN(I)
      ESUM=EINSUM+EKSUM
  295
  300

```

```

301 IF(INCHEKE) 301,305,301
302 ABS(ETOI-ESTUM)-ETENTH) 305,305,302
302 ERONG=1
303 CALL OUTPUT
305 IF(JPROJ=400) 306,306,307
307 JFROJ=300
307 TPRINT=TMAX2
307 TNEXT=T+TPRINT
307 CALL OUTPUT
307 GOTO 121
308 IF(TNEXT-T) 315,315,121
315 CALL OUTPUT
316 TNEXT=TNEXT+TPRINT
316 IF(TMAX-TNEXT+001) 320,121,121
320 TNEXT=TNEXT-TPRINT
320 TPRINT=OUTDT2
320 TNEXT=TNEXT+TPRINT
320 TMAX=5*TMAX
320 IF(XSTP-X(JLAST,NPLUS1)) 556,555,555
556 CALL OUTPUT
556 RETURN

```



```

DC 704 L=1,JLAST1
DO 702 L=2,J(L) 702,703,702
1F(L-INTE(M 4) L'X(L,N)U(L,NMNMHAF),V(L,N),PPLUSQ(L),Q(L,NMNMHAF),
1E(L,N) AREA(L,N),DTSQ(L),X1(L)
1E(L,N) 704
GC TO 704
703 WRITE(M 1H)
5555 FORMAT(1H)
    WRITE(M 14)L,X(L,N)U(L,NMNMHAF),V(L,N),PPLUSQ(L),Q(L,NMNMHAF),
1E(L,N) AREA(L,N),DTSQ(L),X1(L)
704 CNTINUE
    WRITE(M 14) JLAST, X(JLAST,N), U(JLAST,NMNMHAF)
71   WRITE(M 9) IINEQST(I) EKIN(I), EINT(I), I=1,IMAX)
75   WRITE(M 10) NCYCLE,T,DTLAST,ESUM
    WRITE(M 5) FORMATION(IH)
5   FORMAT(1H)
    IF(FWRONG) 95,95,80
80   WRITE(M,11)
95   RETURN
40   FORMAT(1I5,1P7E13.5)
1   FORMAT(5X,12,20H V MODEL LAUNCHER 1413)
2   FFORMAT(1I8H0,J X(J,N) U(J,N-1/2) V(J+1/2,N) P(J+1/2),
1   Q(J+1/2,N-1/2) E(J+1/2,N) AREA(J,N) DTSG((1/2,1/2) DM((J+1/2),
3   FORMAT(1I4H C W CM/MILLISEC(CC/CCO MILLISECSQ GRAMS)
1   BARS BARS-CC/CCO
4   FORMAT(1I4,1P6E13.5) 2E11.3,E13.5)
5   FORMAT(1I5,1P3E15.5) U(J,N-1/2) V(J+1/2,N) P(J+1/2)
1   FORMAT(1I9H0,J X(J,N) U(J,N-1/2) V(J+1/2,N) X(J+1/2,N)
1   Q(J+1/2,N-1/2) E(J+1/2,N) AREA(J,N) DTSG((1/2,1/2) BARS
8   FFORMAT(1I4H C W CM/MILLISEC(CC/CCO MILLISECSQ CM )
1   BARS BARS-CC/CCO
9   FORMAT(46HOREGION MATERIAL K-ENERGY)
10  FORMAT(15,18, 2E15.5)
11  FORMAT(53H T)
12  FORMAT(47HOCYCLE DT
END

```

SSROUTINE CALCUL (EMLEAD)
 CALCULATES INITIAL ENERGY, SPECIFIC VOLUME, AND DENSITY
 COMMON PCQN3,SLOPE,RADIUS,CALPGM,BURND,GMS,PDR,GASPRS,IHEL,
 COMMON AREA1,AREA2,AREA3,AREAF,CQS,CSQMAX,CP,CV,DLAMAX,GUNNO654
 COMMINT,DQ1,DQ2,DLANDA,DTLSQ,DTLAST,DM,ELX,DMUDPDE,GUNNO655
 1DPCMU,DQ1,DQ2,DLANDA,DTLSQ,DTLAST,DM,ELX,DMUDPDE,GUNNO656
 2EWRONG,E1FORCE,GAMMA,HALFM,ESUM,HALFRO,HYDRO1,HYDRO2,HYDRO3,
 4OUTBDY,OUTDT1,OUTDT2,OUTDT3,OUTDT4,OUTDT5,OUTDT6,OUTDT7,OUTDT8,
 5SIGMAX,SIGMIN,SKIN3,MAX2,MAX1,MAX3,MAX4,MAX5,MAX6,MAX7,MAX8,
 6TPRINT,TVNEXT,TMIN3Q,TVFREQ,UZERO,U,USQ,TBAR,TWALL,

C

۶


```

CALL  ZEROB(E,200,2)
CALL  ZEROB(A,200,2)
CALL  ZEROB(Q,200,2)
CALL  ZEROB(U,200,2)
CALL  ZEROB(V,200,2)
CALL  ZEROB(P,200,2)
CALL  ZEROB(X,200,2)
RETURN

SUBROUTINE 1ERO(11,12,13,14,15,16,17,18)
C
Z1=0
Z2=0
Z3=0
Z4=0
Z5=0
Z6=0
Z7=0.
Z8=0.
Z9=0.
Z10=0.
Z11=0.
Z12=0.
Z13=0.
Z14=0.
Z15=0.
Z16=0.
Z17=0.
Z18=0.
Z19=0.
Z20=0.
Z21=0.
Z22=0.
Z23=0.
Z24=0.
Z25=0.
Z26=0.
Z27=0.
Z28=0.
Z29=0.
Z30=0.
Z31=0.
Z32=0.
Z33=0.
Z34=0.
Z35=0.
Z36=0.
Z37=0.
Z38=0.
Z39=0.
Z40=0.
Z41=0.
Z42=0.
Z43=0.
Z44=0.
Z45=0.
Z46=0.
Z47=0.
Z48=0.
Z49=0.
Z50=0.
Z51=0.
Z52=0.
Z53=0.
Z54=0.
Z55=0.
Z56=0.
Z57=0.
Z58=0.
Z59=0.
Z60=0.
Z61=0.
Z62=0.
Z63=0.
Z64=0.
Z65=0.
Z66=0.
Z67=0.
Z68=0.
Z69=0.
Z70=0.
Z71=0.
Z72=0.
Z73=0.
Z74=0.
Z75=0.
Z76=0.
Z77=0.
Z78=0.
Z79=0.
Z80=0.
Z81=0.
Z82=0.
Z83=0.
Z84=0.
Z85=0.
Z86=0.
Z87=0.
Z88=0.
Z89=0.
Z90=0.
Z91=0.
Z92=0.
Z93=0.
Z94=0.
Z95=0.
Z96=0.
Z97=0.
Z98=0.
Z99=0.
Z00=0.

SUBROUTINE 1EROA(1ZA,ZA1,ZA2,ZA3,ZA4,ZA5)
C
DO 1 IZZ=1, 1ZA
ZA1(IZZ)=0.
ZA2(IZZ)=0.
ZA3(IZZ)=0.
ZA4(IZZ)=0.
ZA5(IZZ)=0.

CONTINUE
1 RETURN

END
SUBROUTINE 1EROB(ZAB,1ZA,JZB)
C
DIMENSION ZAB(300)

```

$$\begin{aligned} & \text{DO } 2 \quad IZZ = 1 \quad IZA \\ & \text{DO } 1 \quad JZZ = 1 \quad JZB \\ & ZAB(IIZZ, JZZ) = 0. \\ & \text{CONTINUE} \\ & \text{END} \end{aligned}$$

IND PROQUATINE STOPPIN (ISTOMA) 1

۶

1


```

CONTINUE
  AREA1 = STORM(71)
  AREA2 = STORM(72)
  AREA3 = STORM(73)
  PCCN1 = STORM(74)
  PCCN2 = STORM(75)
  SLPROM = STORM(76)
  EMPROJ = STORM(77)
  QLTD1 = STORM(78)
  QLTD1X1 = STORM(79)
  QLTD1X2 = STORM(80)
  QLTD2 = STORM(81)
  TMAX1 = STORM(82)
  TMAX2 = STORM(83)
  XSTOP = STORM(84)
  XCNCPE = STORM(85)
  SLRADIUS = STORM(86)
  CALPGM = STORM(87)
  TEURND = STORM(88)
  GWSPORE = STORM(89)
  GASPRS = STORM(90)
  EMPIST = STORM(91)
  PWANT = STORM(92)
  PVSLPE = STORM(93)
  PVSLP1 = STORM(94)
  XPVY2 = STORM(95)
  PVERRY = STORM(96)
  PRESRG = STORM(97)
  RETURN

```

```

3 HALF M(200) HALF R(30) HYDRAD(200) INTER J(31) MACH SQ(200) NEQ ST(30) GUN N 0997
4 NZONES(30) OUT BDY(30) PPLUS Q(200) Q(200) R(200) R(200) , GUN N 0998
55 KIN(200) SIG S(200) MIN SQ(200) TO VRE(30) THETA(200) UZER O(30) , GUN N 0999
6U(201) USQ(201) VZE RD(30) V(200) VISCO S(200) X(201,2), X(201,2) , GUN N 1000
72 MASS(200) PO(30) TD(30) AMOL(30) DUMVAR(500,5)
35 HALF R(30) I=1, I MAX
HAL FRO(1)=RZERO(1)/2.

35 INTER J(1)=I MAX
DO 40 I=1,I MAX
INTER J(I+1)=INTER J(I)+NZONES(I)
40 JLAST=INTER J(I MAX+1)

JLAST=JLAST
DO JLAST=JLAST
DNZ CNE=N ZONES(1)
DELX(1)=NZONES(1)
X(1:N)=0.0
U(1:N)=NMN HAF =UZER O(1)
DC 45 I=2,IMAX
DNZ ONE=N ZONES(1)
DELX(I)=(OUT BDY(I)-OUT BDY(I-1))/DNZONE
DC 55 I=1,IMAX
DC IN=INTER J(I+1)-1
JMAX=INTER J(I+1)-1
DC 50 J=JMIN, JMAX
JMN HAF=J-1
U(JMN HAF,N)=UZER O(1)
V(JMN HAF,N)=VZER O(1)
E(JMN HAF,N)=EZER O(1)
F(JMN HAF,N)=EZER O(1)
EX(X(N))=X(N-1,N)+DELX(I)
XX(JMAX+1,N)=OUT BDY(I)
U(JMAX,N)=NMN HAF =UZERO(1)
E(JMAX,N)=EZERO(1)
V(JMAX,N)=VZERO(1)
DO 132 J=1,JLAST
132 CALL ARCOMP
65 DO 130 I=1,IMAX
JMIN=INTER J(I+1)
JMAX=INTER J(I+1)
DC 125 J=JMIN, JMAX
JMN HAF=J-1
120 CALL VCJMP
FAL FM(JMN HAF)=HALF R(1)/V(JMN HAF,N)*VOLUME
125 CCNTINUE
HAL FM(JLAST)=HALF M(JLAST)+EMPROJ
INDEX=NEQ ST(I)
IF(INDEX.EQ.1) CALL EGSI1
IF(INDEX.EQ.2) CALL EGSI2

```

۱۷

```

DIMENSION AREA(200,2),CQSQX4(30),CMAXR(30),CSQ(200),CP(30),CV(30),
DTMIN(30),DLAMA(200),DTSQ(200),DELX(30),DQ(200),DS(200),
DTZERO(30),DE(200),E(200),ENT(30),EK(30),FORCE(30),
HALFM(200),HYDRA(200),INTERJ(30),INT(30),MACHS(200),
NZONE(30),OUTBDY(30),P(200),PPLUSQ(200),PQ(200),
SKIN(200),TSIGSQ(200),TMINUSQ(200),TOVRE(30),TZERO(30),
U(201),USQ(201),V(200),W(200),X(201),Y(200),Z(200),
ZMASS(200),PO(30),PO(30),T(30),AMOL(30),DUMVAR(500,5)

C 120 I=1
125 CONTINUE.
DLAMA=X=0.
SIGMAX=0.
ST=T+DTMIN*(NPPLHAF)
NCYCLE=NCYCLE+1
DO 245 I=1,MAX
N2N=N2NES(I+1)
CYAXR(I)=0.
CSGMAX=0.
JMIN=INTERJ(I)+1
JMAX=INTERJ(I+1)
DO 230 J=JMIN,JMAX
JPLHAF=J-1
JMNHAF=J-1
126 IF(JLAST-J) 155,1700,190
155 DUDT=PPLUSQ(JMNHAF)*AREA(JLAST,N)/(HALFNM(JMNHAF))
IF(JPROJ-EQ.300.AND.E(JMNHAF,N).NE.0.0) GC TO 195
GO TO 901
1700 IF(JPROJ-EQ.300) GO TO 1755
IF(J.EQ.1)INTERJ(6) GO TO 901
GC TO 1755
IF(PPLUSQ(JMNHAF)-SHPR) 902,903,903
902 I=JNPPLHAF=0.0
903 GC TO 196
JPROJ=500
1755 DTSQ(200)=T
IF(J.EQ.JMAX.AND.NZN.EQ.1) GO TO 876
IF(J.EQ.JMAX.AND.NZN.GT.1) GO TO 800
DUDT=(PPLUSQ(JMNHAF)-PPLUSQ(JPLHAF)) * AREA(J,N)/(HALFNM(JMNHAF)) +
1 HALFM(JPLHAF)
1 GC TO 195
800 IF(J.EQ.1)INTERJ(6) GO TO 863
DUDT=-(1.5*(PPLUSQ(JMNHAF)-(JPLHAF))-PPLUSQ(JPLHAF+1))-
1 PPLUSQ(JMNHAF-1)/6.* AREA(J,N)/(HALFNM(JMNHAF)+(JPLHAF)) -
1 GC TO 195
863 DUDT=-(1.5*(PPLUSQ(JPLHAF)-(PPLUSQ(JMNHAF))-(PPLUSQ(JMNHAF-1))-
1 (PPLUSQ(JMNHAF)/3.+2.*PPLUSQ(JMNHAF-1)/3.-
1 )/6.* AREA(J,N)/(HALFNM(JMNHAF)+(JPLHAF)) -

```

```

1 94 IF(T.GE.(DTSQ(200)+DTSQ(199)) ) GO TO 194
DUDT=DUDT*(T-DTSQ(200))/DTSQ(199) GO TO 194
CONTINUE
1 95 GO TO 1 95
876 A=2.*HALFM(JMNHAF)+HALFM(JPLHAF)
B=HALFM((2.*A**2.*PPLUSQ(JPLHAF))
DUDT=((2.*A**2.*PPLUSQ(JPLHAF))
1-(A-B)*(A+B)*PPLUSQ(LMNHAF)
2+(A-B)*PPLUSQ((JMNHAF-1))
1/(A*(A+B)*B)*(-1.)*AREA(J,N)
1 95 U(J,NPLHAF)=U(J,JMNHAF)+DTMIN(NN)*DUDT
X(J,NPLUS1)=X(J,N)+DTMIN(NPLHAF)*U(J,NPLHAF)
CALL ARCOMP
CALL VCOMP
V(JMNHAF,NPLHAF)=HALF((JMNHAF)*VOLUME
1 96 IF((U(J,NPLHAF)-U(J-1,NPLHAF)) 205 225 225
Q(JMNHAF,NPLHAF)=CQSQ(X4(I)*HALF((I)*(U(J,NPLHAF,N)
1#*2/(V(JMNHAF,NPLUS1)+V(JMNHAF,N))
1 96 GO TO 230
225 C(JMNHAF,NPLHAF)=0.
230 CONTINUE
INDEX=NEQST(I)
IF(INDEX.EQ.1)CALL ECST1
IF(INDEX.EQ.2)CALL ECST2
IF(INDEX.EQ.3)CALL ECST3
53 DO 240 J=JMIN,JMAX
JMNHAF=J-1
IF(JPRU*LT*300*AND*J.GT.INTERJ(6)) GO TO 24
TSIGSQ(JMNHAF)=CSQ(JMNHAF)/(X(J,NPLUS1)-X(J-1,NPLUS1))**2
24 CONTINUE
PPLUSQ(JMNHAF)=P(JMNHAF)/NPLUS1+Q(JMNHAF,NPLHAF)
DLAMDA(JMNHAF)=CQSQ(X4(I)/2*(V(JMNHAF,NPLHAF)
1*(V(JMNHAFN)+V(JMNHAFN)/NPLUS1))-V(JMNHAF,NPLUS1))/
CHANGED T0 MAX1 JANUARY 16 1967 DKS
DLAMAX= MAX1(DLAMDA(JMNHAF),DLAMAX)
CSCMAX= MAX1(TSIGSQ(JMNHAF),SIGMAX)
IF((TSIGSQ(JMNHAF)=MAX1(CSQMAX,X(CSQMAX,CSQ(JMNHAF)))
DTSQ(JMNHAF)=0.0) GO TO 240
245 GTSQ(JMNHAF)=SQR((CSQMAX)
245 CONTINUE
245 RETURN
END
SUBROUTINE ARCOMP SECTIONAL AREA
DETERMINE ZONE CROSS SECTIONAL AREA
COMMON PCON3,SLOPE,RADIUS,CALPGM,TBURND,GMS,FDR,GASPRS,IHEL
COMMON AREA1,AREA2,AREA3,AREA,CQSQX4,CMAXR,CSQ,CSQMAX,CP,CV,DLAMAX,GUNN

```

۶

```

2E ZERO(30) E(200,2) EINT(30) EKIN(30) FORCE(200) GAMMA(30)
3F ALFM(200) HALFRD(30) HYDRAD(200) INTERJ(31) HSQ(200) NEQST(30)
4 ANZONES(30) OUTBDY(30) PPLUSQ(200) P(200,2) Q(200,2) R0ZERO(30),
5 SKIN(200) TSIGSQ(200) TMINSQ(200) T(200,2) T(200,2) TETRA(30),
6 U(201,2) USQ(201) V(200,2) V(200,2) VISCOS(200), X(201,2), X(200,1),
7 ZMASS(200), YZERO(30), ZZERO(30), PO(30), TD(30), DUMVAR(500,5)
XPV1=0.
XPV2=0.
PVERR=0.
PRESCG=0.
1 IF(X(J,NPLUS1)-PCON1) * AREA1
2 3 VOLUME=(X(J,NPLUS1)-X(J,NPLUS1)) * AREA1
4 4 IF(X(J-1,NPLUS1)-PCON1) * AREA2
5 5 VOLUME=(X(J,NPLUS1)-PCON1) * AREA2+(PCON1-X(J-1,NPLUS1)) * AREA1
6 6 GOTO 17
7 7 GO TO 17
8 8 IF(X(J,NPLUS1)-PCON3) * AREA2
9 9 IF(X(J-1,NPLUS1)-PCON2) * AREA1
10 10 VOLUME=(X(J,NPLUS1)-X(J-1,NPLUS1)) * AREA2
11 11 VOLUME=(X(J,NPLUS1)-X(J-1,NPLUS1)) * AREA1
12 12 IF(X(J-1,NPLUS1)-PCON3) * AREA2
13 13 VOLUME=(X(J,NPLUS1)-X(J-1,NPLUS1)) * AREA3
14 14 IF(X(J-1,NPLUS1)-PCON2) * AREA3
15 15 VOLUME=(X(J,NPLUS1)-X(J-1,NPLUS1)) * AREA3
16 16 VOLUME=(X(J,NPLUS1)-X(J-1,NPLUS1)) * AREA3
17 17 END
SUBROUTINE EQST1
CALCULATES PRESSURE AND ENERGY FOR IDEAL GAS ZONES
COMMON PCON3,SLOPE,RADIUS,CALPGM,TBURN,GMSPDR,GASPRS,IHEL,
COMMON AREA1,AREA2,AREA3,AREAT,CQS,QX4,CMAX,XG,DLAMAX,XG,
COMMON DUDT,DLAMDA,DTSQ,DTLAS,DTSQ,DLAS,DTSQ,DLAS,DTSQ,
COMMON DCL,DQ2,DS,EZERO,EINSUM,ESUM,HALF,HALF,HALF,HALF,
COMMON DPMU,DC1,DC2,DS,EZERO,EINSUM,ESUM,HALF,HALF,HALF,HALF,
COMMON DWRONG,E1,FORCE,GAMMA,PCON1,PCON2,PCON1,PCON2,PCON1,
COMMON OUTDT1,OUTDT2,OUTDT3,OUTDT4,OUTDT5,OUTDT6,OUTDT7,
COMMON SIGMAX,SIGMIN,TMAX,TMAX,TMAX,TMAX,TMAX,TMAX,TMAX,
COMMON TPRINT,TVNEXT,TMAX,TMAX,TMAX,TMAX,TMAX,TMAX,TMAX,
COMMON TZERO,VOLUME,VOLUME,VOLUME,VOLUME,VOLUME,VOLUME,VOLUME,
COMMON IMAX,INU,INTERJ,INDEX,ILIMIT,JPROJ,JPROJ,JMAX,J,
COMMON JPLHAF,JMNHAF,JLAST,JLAST,JLAST,JLAST,JLAST,JLAST,J,
COMMON INDATE3,NUMBER,NTV,NCHKE,NEQST,NZONES,NCYCLE,N,NMHAF,NPLUSI,
COMMON C

```

6

```

1 BURND=0
2 TOLDE=0
3 TINTERS=2001=2
4 GASPRS=GASPRS*GASPRS/1000
5 PVOL=PCON1*AREAL*001-PVOL
6 GMOLESS=GMSPDR*GSPDR/24.61
7 PRESUR=(GMOLESS+PMOLESS)*24.61/(PVOL+PVOL)*1.0138
8 IF(IHEL)40=14040
9 GAMMA(I)=(GMOLESS*1.667+PMOLESS*1.23)/(GMOLESS+PMOLESS)
10 WGTMOL=(GMOLESS*4.0026+PMOLESS*25.1)/(GMOLESS+PMOLESS)
11 GO TO 50
12 GAMMA(I)=(GMOLESS*1.4+PMOLESS*25.0)/(GMOLESS+PMOLESS)
13 WSPCVOL=(83.17*300.0/WGTMOL)/PRESUR*WGTMOL
14 ROZERO(I)=SPCVOL*ROZERO(I)
15 VZERO(I)=PRESUR*VZERO(I)
16 FZERO(I)=PRESUR*VZERO(I)/(GAMMA(I)-1.)
17 JMIN1=JMIN-1
18 JMAX1=JMAX-1
19 DO 20 J=JMIN1 JMAX1
20 E(J,N)=EZERO(I)
21 V(J,N)=VZERO(I)
22 PEAK=CALPGM*41.84*ROZERO(I)*PMOLESS*25.0/(PMOLESS*25.0)
23 HALFRO(I)=ROZERO(I)/2.
24 DC30 J=JMIN JMAX
25 VOLUME=(X(J,N)-X(J-1,N))*AREAL
26 HALFM(J-1)=HALFRO(I)/V(J-1,N)*VOLUME
27 JMIN1=JMIN-1
28 JMAX1=JMAX-1
29 IF(TBURN1)4,7,7
30 IF(TBURN1)4,7,7
31 STATEMENT IF(TBURN1 EQ. 0.0) GO TO 6
32 VERTBURN1=635
33 DELE=PEAK*(T-TOLD)/TBURN1
34 TOLD=T
35 GO TO 7
36 DELE=0
37 DO 10 JMNHAJ=JMIN1 JMAX1
38 E1=E(JMNHAJ N)-(P(JMNHAJ, N)+Q(JMNHAJ, N))* (V(JMNHAJ, NPLUS1))-GUNN1375
39 1V(JMNHAJ N)+DELE
40 P1=(GAMMA(I)-1)*E1/V(JMNHAJ, NPLUS1)
41 E(JMNHAJ, NPLUS1)=E1-5*(P1-P(JMNHAJ, N))* (V(JMNHAJ, NPLUS1))-GUNN1376
42 1V(JMNHAJ, N)

```

6

```

IF (ABS(AVEL(N)-PVW)•LT•ERR) GO TO 30
IF (AVEL(N)•GT•PVW•AND•AVEL(N)•LT•PVHI) GO TO 20
IF (AVEL(N)•LT•PVW•AND•AVEL(N)•LT•PVLO) GO TO 40
IF (AVEL(N)•LT•PVW) GO TO 40
HLOAD=ALOAD(N)
PVHI=AVEL(N)
GO TO 20
BALOAD=ALOAD(N)
PVLO=AVEL(N)
CONTINUE
IF (PVLO•EQ•10•OR•PVHI•EQ•5000•)*(BALOAD-HLOAD)/(PVLO-PVHI)
PLOAD=BALOAD+(PVW-PVLO)*(BALOAD-HLOAD)/(PVLO-PVHI)
GO TO 50
ALOAD=ALOAD(N)
GO TO 50
PLOAD=PLOAD +(PVW-VEL)* 20.
GAS(1)=PLOAD
RETURN
END

```

GUNN1429
GUNN1430
GUNN1431
GUNN1432
GUNN1433
GUNN1434
GUNN1435
GUNN1436
GUNN1437
GUNN1438
GUNN1439
GUNN1440
GUNN1441
GUNN1442
GUNN1443
GUNN1444
GUNN1445
GUNN1446
GUNN1447

INPUT FORMAT

CARD 1 (4I3,FI0.0)
IDATA = 0, STANDARD 18 CARD INPUT
= NAMELIST INPUT OF ALL VARIABLES ON CARDS
IPRNTZ = 0, STANDARD RUN
= 1, PRINT OUT INITIAL DATA ONLY
INTRNSF = 0, USE DISK SCRATCH FILE AND PRINT OUT ONLY LAST PISTON ITERATION
= 1, PRINT OUT ALL PISTON ITERATIONS (HYPERVELOCITY MODEL ONLY)
IPUNCH = 0, NO PUNCHED OUTPUT
= 1, PUNCHED OUTPUT OF MODEL BASE PRESSURE VS TIME
DTSQ(199) FINITE BREAK VALVE OPENING TIME

CARD 2 (20I3)
IMAX = NUMBER OF REGIONS (UP TO SIX)
NDATE1 = MONTH
NDATE2 = DAY
NDATE3 = YEAR
NUMBER = RUN IDENTIFICATION NUMBER
NCHEKE = 0, NO ENERGY CHECK
= 1, ENERGY MONITORED AND PROBLEM STOPPED IF THE TOTAL ENERGY
CHANGES BY MORE THAN 10%
INU = 0, ALL ZONES HAVE ZERO INITIAL VELOCITY
= 1, ALLOWS INITIAL VELOCITY FOR EACH ZONE TO BE READ
JPROJ = MASS POINT NUMBER OF PROJECTILE

CARD 3 (2013)
NEQST(I) = NUMBER OR INDEX OF EQUATION OF STATE USED IN REGION I

CARD 4 (2013)
NZONES(I) = NUMBER OF ZONES IN REGION I

CARD 5 (7F10.0)
OUTBDY(I) = DISTANCE IN CM TO OUTER INTERFACE OF REGION I

CARD 6 (7F10.0)
GAMMA(I) = RATION OF SPECIFIC HEATS FOR REGION I

CARD 7 (7F10.0)
CQSQX4(I) = CONSTANT USED IN ARTIFICIAL VISCOSITY COMPUTATION
(GOOD VALUES ARE 4.0 FOR GAS REGION, 9.0 FOR SOLID REGION)

CARD 8 (7F10.0)
AREA1 = AREA IN SQ CM OF FIRST CONSTANT AREA SECTION (PROGRAM ALLOWS UP TO
THREE DIFFERENT CONSTANT AREA SECTIONS AND ONE TAPERED SECTION
BETWEEN THE SECOND AND THIRD CONSTANT AREA SECTIONS)
AREA2 = AREA IN SQ CM OF SECOND CONSTANT AREA SECTION
AREA3 = AREA IN SQ CM OF THIRD CONSTANT AREA SECTION
PCON1 = POSITION IN CM WHERE FIRST AREA CHANGE OCCURS
SHPR = PROJECTILE RELEASE PRESSURE IN BARS
EMPROJ = MASS OF PROJECTILE IN GRAMS

OUTDT1 = DELTA T FOR PRINTING UP TO TIME TMAX1
TMAX1 = MILLISECS
OUTDT2 = DELTA T FOR PRINTING UP TO TIME TMAX2
TMAX2 = MILLISECS
XSTOP = POSITION IN CM THAT WHEN THE INTERFACE JSTOP REACHES IT,
THE PROBLEM IS TERMINATED

CARD 9 (7F10.0) REQUIRED ONLY IF INU = 1
UZERO(I) = INITIAL VELOCITY FOR EACH ZONE

CARD 10 (7F10.0)
PCON = POSITION IN CM WHERE THIRD AREA CHANGE OCCURS
SLOPE = SLOPE OF CONSTANT TAPERED SECTION
RADIUS = RADIUS IN CM OF THE CONSTANT AREA SECTION TO THE RIGHT
OF THE TAPERED SECTION

CARD 11 (4F10.0I4)
CALPGM = CALORIES PERGRAM OF POWER
TBURND = TIME TO BURN POWDER
GMSPDR = GRAMS OF POWDER
GASPRS = INITIAL GAS PRESSURE IN POWDER REGION
IHEL = 0 (NOT APPLICABLE TO GUN PROJECT)

CARD 12 (7F10.0)
IPOX = 0 ALL PLOTS, ALL PRESSURE POINTS (PLOT ROUTINE MUST BE INCLUDED)
= 1 ALL PLOTS, NO PRESSURE POINTS
= 5 NO PLOTS, NO PRESSURE POINTS
= 6 ONLY PRESSURE POINTS
NPOX = NUMBER OF PRESSURE POINTS (UP TO FIVE)
XPO(1) = X POSITION IN CM OF PRESSURE POINT 1

CARD 13 (7F10.0) HYPERVELOCITY MODEL LAUNCHER PARAMETERS, (NOT APPLICABLE
TO GUN PROJECT)
XPV1 = X POSITION IN CM OF FIRST MEASUREMENT POINT OF PISTON VELOCITY
XPV2 = X POSITION IN CM OF SECOND MEASUREMENT POINT OF PISTON VELOCITY
PVERR = PISTON VELOCITY ERROR IN FT PER SEC
PVWANT = DESIRED PISTON VELOCITY IN FT PER SEC

CARD 14 (E10.0, 3F10.0)
R = 8317E 08 GAS CONSTANT
EMPIST = MASS OF FIRST PISTON SECTION (HYPERVELOCITY MODEL LAUNCHER ONLY)
FRAC = 1.0
EMLEAD = MASS OF SECOND PISTON SECTION (HYPERVELOCITY MODEL LAUNCHER)

CARD 15 (7F10.0)
PO(1) = INITIAL PRESSURE IN PSI IN REGION 1

CARD 16 (7F10.0)
TO(1) = INITIAL TEMPERATURE IN DEGREES KELVIN IN REGION 1

AD-A032 366 NAVAL POSTGRADUATE SCHOOL MONTEREY CALIF
APPLICATION OF HOLOGRAPHIC INTERFEROMETRY TO THE INTERIOR BALLI--ETC(U)
SEP 76 R L MONTGOMERY

F/G 20/6

NL

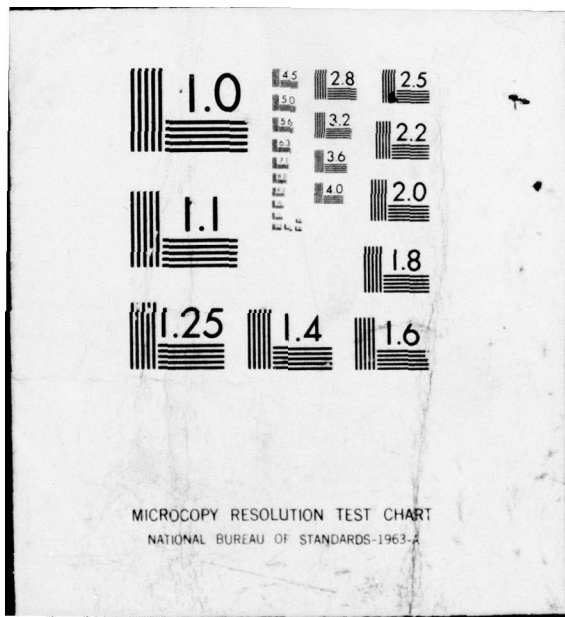
UNCLASSIFIED

2 OF 2
AD
A032 366



END

DATE
FILMED
1 - 77



CARD 17 (7F10.0)
AMOL(I) = MOLECULAR WEIGHT OF MATERIAL IN REGION I

CARD 18 (13)
ILASTK = 0, STOP
= 1, CONTINUE FOR NEW RUN

LIST OF REFERENCES

1. Corner, J., Theory of the Interior Ballistics of Guns, Wiley and Sons, 1950.
2. Gough, P. S., Fundamental Investigations of the Interior Ballistics of Guns, North Troy, Vermont, 1974.
3. Smith, H. M., Principles of Holography, Wiley and Sons, 1969.
4. Collier, R., Burckhardt, C. B., and Lin, L. H., Optical Holography, Academic Press, New York, 1971.
5. Naval Ordnance Laboratory Technical Report 62-87, Ballistics Research Report 67, 1963, Computer Analysis of Two-Stage Hypervelocity Model Launchers, by R. Piacesi, D. F. Gates, and A. E. Seigel.
6. Richtmyer, R. D., Difference Methods for Initial Value Problems, Interscience Publishers, Inc., New York, 1957.
7. VanNeumann, J., and Richtmyer, R. D., "A Method for Numerical Calculation of Hydrodynamic Shocks," Journal of Applied Physics, V. 21, P. 232, 1950.
8. Bettinger, R. G., Application of Holographic Interferometry to the Exterior Ballistic Flow Field in the Muzzle Environment of a Twenty Millimeter Cannon, Thesis, Naval Postgraduate School, 1975.
9. Richtmyer, R. D., Difference Methods for Initial Value Problems, Interscience Publishers, Inc., New York, 1957.
10. Hunt, F. R. W., Internal Ballistics, Philosophical Library, Inc., 1951.

INITIAL DISTRIBUTION LIST

	No. Copies
1. Defense Documentation Center Cameron Station Alexandria, Virginia 22314	2
2. Library, Code 0212 Naval Postgraduate School Monterey, California 93940	2
3. Department Chairman, Code 67 Department of Aeronautics Naval Postgraduate School Monterey, California 93940	1
4. Professor D. J. Collins, Code 67Co Department of Aeronautics Naval Postgraduate School Monterey, California 93940	2
5. LT Richard L. Montgomery, USN 217 Broadway Fort Edward, New York 12828	1
6. Professor D. W. Netzer, Code 67Nt Department of Aeronautics Naval Postgraduate School Monterey, California 93940	1
7. Mr. Michael Lamb Naval Ordnance Station, Code 50326 Indian Head, Maryland 20640	2